U.S.N.A. --- Trident Scholar project report; no. 294 (2002)

CHARACTERIZATION OF AN OPTICAL SELF-HOMODYNE DPSK RECEIVER
by

Midshipman Tarek Elmasry, Class of 2002
United States Naval Academy
Annapolis, Maryland

_____
(signature)

_____
(date)

Certification of Adviser(s) Approval

Associate Professor Brian Jenkins
Electrical Engineering Department

_____
(signature)

_____
(date)

Associate Professor Deborah Mechtel
Electrical Engineering Department

_____
(signature)

_____
(date)

Acceptance of the Trident Scholar Committee

Professor Joyce E. Shade
Deputy Director of Research & Scholarship

_____
(signature)

_____
(date)

USNA-1531-2

REPORT DOCUMENTATION PAGE

Form Approved OMB No. 0704-0188

1. REPORT DATE (DD-MM-YYYY) 02-05-2002	2. REPORT TYPE	3. DATES COVERED (FROM - TO) xx-xx-2002 to xx-xx-2002

4. TITLE AND SUBTITLE
Characterization of an Optical Self-Homodyne DPSK Receiver
Unclassified

5a. CONTRACT NUMBER
5b. GRANT NUMBER
5c. PROGRAM ELEMENT NUMBER

6. AUTHOR(S)
Elmasry, Tarek ;

5d. PROJECT NUMBER
5e. TASK NUMBER
5f. WORK UNIT NUMBER

7. PERFORMING ORGANIZATION NAME AND ADDRESS
US Naval Academy
Annapolis, MD21402

8. PERFORMING ORGANIZATION REPORT NUMBER

9. SPONSORING/MONITORING AGENCY NAME AND ADDRESS
,

10. SPONSOR/MONITOR'S ACRONYM(S)
11. SPONSOR/MONITOR'S REPORT NUMBER(S)

12. DISTRIBUTION/AVAILABILITY STATEMENT
APUBLIC RELEASE
,

13. SUPPLEMENTARY NOTES

14. ABSTRACT
See report

15. SUBJECT TERMS

16. SECURITY CLASSIFICATION OF:	17. LIMITATION OF ABSTRACT Public Release	18. NUMBER OF PAGES 50	19. NAME OF RESPONSIBLE PERSON email from USNA, Annapolis, MD, (blank) lfenster@dtic.mil

| a. REPORT Unclassified | b. ABSTRACT Unclassified | c. THIS PAGE Unclassified | | | 19b. TELEPHONE NUMBER International Area Code Area Code Telephone Number 703767-9007 DSN 427-9007 |

Standard Form 298 (Rev. 8-98)
Prescribed by ANSI Std Z39.18

REPORT DOCUMENTATION PAGE

Public reporting burden for this collection of information is estimated to average 1 hour per response, including g the time for reviewing instructions, searching existing data sources, gathering and maintaining the data needed, and completing and reviewing the collection of information. Send comments regarding this burden estimate or any other aspect of the collection of information, including suggestions for reducing this burden to Washington Headquarters Services, Directorate for Information Operations and Reports, 1215 Jefferson Davis Highway, Suite 1204, Arlington, VA 22202-4302, and to the Office of Management and Budget, Paperwork Reduction Project (0704-0188), Washington, DC 20503.

1. AGENCY USE ONLY (Leave blank)	2. REPORT DATE 2 May 2002	3. REPORT TYPE AND DATE COVERED

4. TITLE AND SUBTITLE
Characterization of an optical self-homodyne DPSK receiver

5. FUNDING NUMBERS

6. AUTHOR(S)
Elmasry, Tarek (Tarek Sameh), 1980-

7. PERFORMING ORGANIZATION NAME(S) AND ADDRESS(ES)

8. PERFORMING ORGANIZATION REPORT NUMBER

9. SPONSORING/MONITORING AGENCY NAME(S) AND ADDRESS(ES)
US Naval Academy
Annapolis, MD 21402

10. SPONSORING/MONITORING AGENCY REPORT NUMBER
Trident Scholar project report no. 294 (2002)

11. SUPPLEMENTARY NOTES

12a. DISTRIBUTION/AVAILABILITY STATEMENT
This document has been approved for public release; its distribution is UNLIMITED.

12b. DISTRIBUTION CODE

13. ABSTRACT: The goal of this project was to create a digital optical demodulator capable of processing information propagating at high data rates in an optical fiber. By processing data at higher rates the information capacity of the channel can be increased. Most demodulators in commercial applications utilize electrical systems. When an optical signal propagating in a fiber optic channel arrives at the receiver, the optical to electrical signal conversion can significantly slow down the processing speed. By optically processing the signal just before the electrical receiver, information can be transmitted at higher data rates. Many methods of building an optical demodulator have been tried using different digital signal processing techniques. In this project a demodulator was designed for differential phase shift keyed (DPSK) data using self-homodyne coherent detection, without using a local oscillator. Local oscillators are often incorporated into coherent receivers to provide a phase reference for incoming data. By replacing the local oscillator with a 3-dB coupler and a delay line, the design of this receiver was simplified. In this configuration the incoming signal uses itself as the reference. Past work on this topic has been mostly theoretical. This project went further by successfully testing a hardware model. Much of the experimental work concentrated on ensuring that constructive and destructive interference occurred in 3-dB couplers. The receiver setup was extremely sensitive to vibration. Experiments had to be performed on a floating table and the receiver had to be enclosed to give proper environmental isolation. In addition to hardware testing of this receiver, computer simulation of the model was performed to determine required component parameters. It was found that the dominant limiting factor of the communication system was the line width of the laser. However, attenuation and receiver noises were also found to have pronounced effects on performance if they exceeded certain limits.

14. SUBJECT TERMS
DPSK, Optical, Coherent, Phase noise

15. NUMBER OF PAGES
50

16. PRICE CODE

17. SECURITY CLASSIFICATION OF REPORT	18. SECURITY CLASSIFICATION OF THIS PAGE	19. SECURITY CLASSIFICATION OF ABSTRACT	20. LIMITATION OF ABSTRACT

Abstract

The goal of this project was to create a digital optical demodulator capable of processing information propagating at high data rates in an optical fiber. By processing data at higher rates the information capacity of the channel can be increased. Most demodulators in commercial applications utilize electrical systems. When an optical signal propagating in a fiber optic channel arrives at the receiver, the optical to electrical signal conversion can significantly slow down the processing speed. By optically processing the signal just before the electrical receiver, information can be transmitted at higher data rates. Many methods of building an optical demodulator have been tried using different digital signal processing techniques. In this project a demodulator was designed for differential phase shift keyed (DPSK) data using self-homodyne coherent detection, without using a local oscillator. Local oscillators are often incorporated into coherent receivers to provide a phase reference for incoming data. By replacing the local oscillator with a 3-dB coupler and a delay line, the design of this receiver was simplified. In this configuration the incoming signal uses itself as the reference.

Past work on this topic has been mostly theoretical. This project went further by successfully testing a hardware model. Much of the experimental work concentrated on ensuring that constructive and destructive interference occurred in 3-dB couplers. The receiver setup was extremely sensitive to vibration. Experiments had to be performed on a floating table and the receiver had to be enclosed to give proper environmental isolation.

In addition to hardware testing of this receiver, computer simulation of the model was performed to determine required component parameters. It was found that the dominant limiting factor of the communication system was the linewidth of the laser. However, attenuation and receiver noises were also found to have pronounced effects on performance if they exceeded certain limits.

**Key Words:** DPSK, Optical, Coherent, Phase Noise

Table of Contents

I. Introduction

The purpose of a communication system is to transmit information from one place to another. In this paper, an optical communication system using differential phase shift keying (DPSK) is discussed and tested. A communication system consists of three primary components: a transmitter, a channel, and a receiver. The transmitter information may be either analog or digital. Digital communication systems are addressed in this paper.

Figure 1.1 (The Basic Communication System)
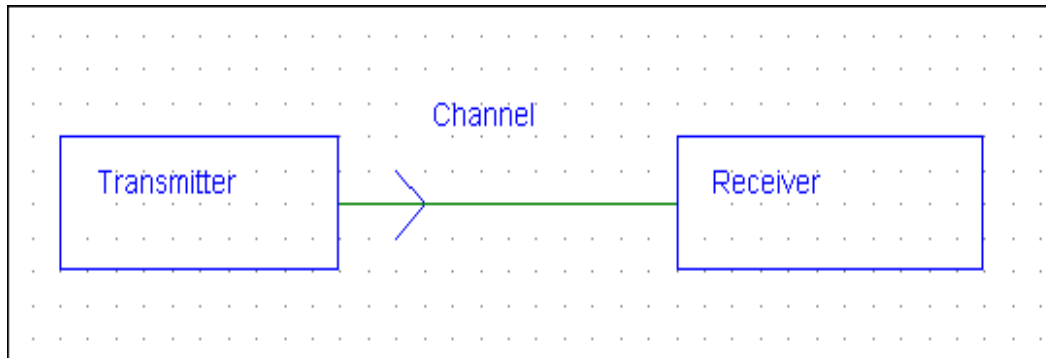
Traditional communication systems are electrical. However, in recent years, integration of fiber optics into communication systems has become popular due to several advantages it offers. The primary advantage is bandwidth. Bandwidth is an important property of a communication system. It is the range of frequencies over which information may be transmitted and received. At the transmitter, information must be modulated onto an optical wave and transmitted at a specific frequency. Optical communication systems offer a much larger bandwidth (5 orders of magnitude greater) than electrical systems. [1] Through wavelength division multiplexing (WDM), multiple channels can be transmitted simultaneously over a single fiber link, dramatically increasing channel capacity beyond that possible with a single wavelength.

A. Coding and Decoding

In a digital communication system, information is often sent as a binary stream of data where the fundamental unit of data is a bit. In a binary system a bit assumes one of two possible values (0 or 1). In many communication systems, including this one, the bit sequence is first encoded before it is transmitted. The information in this proposed communication system employs differential encoding. Differential encoding defines and uses a relationship between consecutive bits in a bit stream to encode a sequence. Differential encoding takes in a bit sequence "B" and performs an exclusive nor (XNOR) logic operation between two bits

Table 1.1 (Truth Table for "Exclusive Nor" Operation)

Input 1	Input 2	XNOR
0	0	1
0	1	0
1	0	0
1	1	1

(see Table 1.1) to produce a differentially coded sequence, "D". The first bit in a differentially coded sequence is obtained by assigning a reference bit (gray box in Table 1.2) and performing an XNOR operation with the first bit in sequence "B." Successive bits are obtained by performing an XNOR operation between the next un-coded bit in "B" and the previously coded bit in sequence "D." Table 1.2 shows an example of differential coding where the reference bit has been chosen to be a '0'. As a sample calculation, the differential sequence value in column four (blue box) is obtained by taking the bit stream value in column four (red box) and performing an XNOR operation with the differential sequence value in column three (green box).

Table 1.2 (Example of Differential Encoding)

Column number	1	2	3	4	5	6	7	8	9	10	11
Un-coded Sequence "B"		0	1	1	1	0	1	0	0	1	0
Differential Sequence "D"	0	1	1	1	1	0	0	1	0	0	1

To recover the coded sequence, a differential decoding operation needs to be performed. Differential decoding also uses the exclusive nor (XNOR) operation. If "D" is a differentially coded sequence, then the decoded sequence "B" will be recovered. To decode a differential sequence, it must be first delayed by one bit relative to itself. This is shown in Table 1.3. As with encoding, decoding a differential sequence requires a reference bit, shown in the gray box of Table 1.3. The reference bit must be the same reference bit used to encode the sequence. Table 1.3 gives an example of differential decoding. The XNOR operation is performed on the red and green boxes to yield the blue box output. Comparing Table 1.3 to Table 1.2 shows the decoded sequence to be the same as the original sequence.

Table 1.3 (Example of Differential Decoding)

Column number	1	2	3	4	5	6	7	8	9	10	11
Differential Sequence "D"	1	1	1	1	0	0	1	0	0	1	
Delayed Differential Sequence "$D_{de;}$"	0	1	1	1	1	0	0	1	0	0	1
Decoded Sequence "B"	0	1	1	1	0	1	0	0	1	0	

## B. Phase Modulation and DPSK

In coherent optical communications the electric field of light is modulated to send information. In its simplest form, the time-varying electric field of coherent light is represented by:

$$E(t) = A\sin(2\pi ft + \phi)$$ (1.1)

where A is the amplitude, f is the frequency, and ϕ is the phase of the electric field. Any one of these three parameters can be modulated to send a signal. In this system phase modulation is used. In phase modulation, ϕ varies while A and f remain constant. Thus a differentially coded sequence can be represented by the electric field of an optical signal using phase modulation. By modulating the phase of the electric field so that it assumes only two values, the phase information is binary. Figure 1.2 shows an example of a binary phase shift keyed bit stream. In the bit periods where $\phi = 0$, a '0' has been transmitted and in the periods where $\phi = \pi$, a '1' has been transmitted so that the bit sequence from this figure is 00101. Transmission of a phase modulated differentially encoded sequence is also known as DPSK.

Figure 1.2 (Example of Phase Shift Keying)
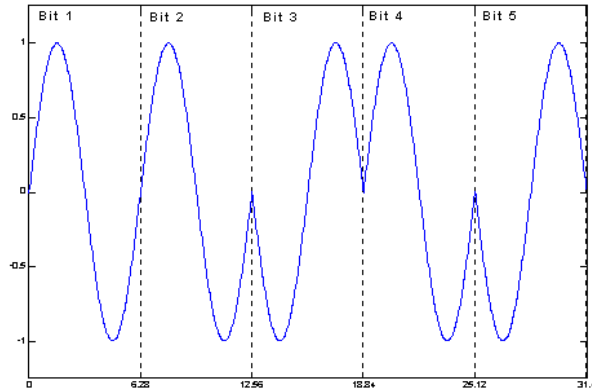
C. System Challenges and Advantages

This communication system optically decodes a differentially encoded stream at the receiver. In the transmitter, a phase modulator produces a differentially encoded sequence that controls a pulse generator. In order to decode the sequence at the receiver, phase information from the received electrical field must be extracted. Testing devices that measure the optical power of a signal directly, yield no phase information. However, the interference between two optical signals is phase dependent, permitting indirect phase information extraction. This communication system uses this principle in receiver design. Optical signals in a practical environment encounter difficulties (discussed in following sections) which make it difficult to generate the proper interference effects. The proposed communication system seeks to overcome these difficulties in a lab environment.

Other forms of modulation exist other than DPSK. Other commonly used formats include frequency shift keying (FSK) and amplitude shift keying (ASK). There is also multilevel signaling as in M-ary keying formats. Discussion in this paper is limited to binary modulation systems. The choice of DPSK as the modulation format in this system is based on the belief that it simplifies receiver design while simultaneously offering superior performance. Stremler showed that the theoretical performance of a receiver using a DPSK format is exceeded only by that offered in a PSK receiver. [2] However, PSK receivers are more complex than the receiver proposed in this paper. Recently, a communication system using a DPSK format achieved a new transmission distance record by transmitting 2.5 Tb/s over a $4*10^6$ m channel. In this system 64 channels each transmitting at 42.7 Gb/s were used to achieve the record. [3]

II. Theory

A. The Ideal Theoretical Model

i. Qualitative Description

Figure 2.1 shows the basic block diagram of the communication system. This design is based heavily on prior research by Kiasaleh [4], and others [5]-[9]. Before discussing the mathematical details of this system, a brief qualitative description is given. The transmitter is on the left side of Figure 2.1. The central component of the transmitter is a phase modulator, which has two inputs. One of the inputs is the output from a continuous wave (CW) laser diode. The other input is an electrical waveform corresponding to a differentially encoded bit stream generated by a pulse generator. The pulse generator consists of three components. The first component generates a Pseudo Random Binary Sequence (PRBS)[1], the second component differentially encodes the sequence, and the third component produces a non-return to zero (NRZ) electrical waveform of the differentially coded sequence, which is passed on to the phase modulator. At the phase modulator the electric signal from the pulse generator is used to

Figure 2.1 (System Block Diagram)
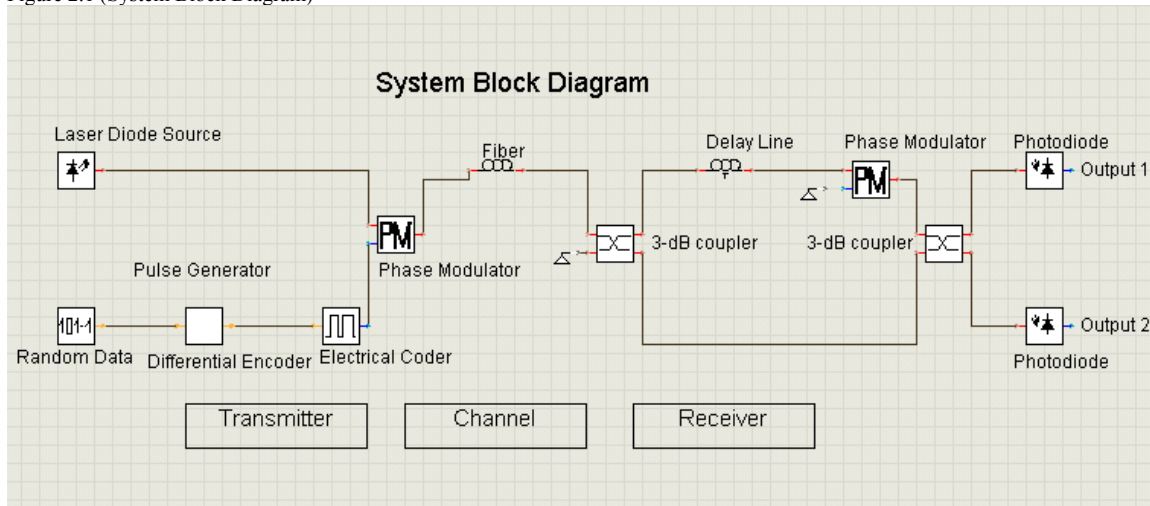
modulate the phase of a continuous wave laser, producing a phase modulated optical signal. The optical signal then propagates through the channel, a fiber optic cable, and arrives at the receiver. The receiver consists of multiple components. The first component in the receiver is a 3-dB coupler which splits the input signal power equally to produce two output optical signals. Splitting the input signal produces a reference signal. One of the coupler output signals is delayed in time relative to the other output signal, phase modulated and then passed on to a second 3-dB coupler. The other coupler output directly travels to the second 3-dB coupler. Properly delaying and phase modulating one of the signals in between the two couplers creates the conditions needed for proper optical interference to take place. This interference takes place in the second coupler. As a result of proper interference occurring, the second coupler generates

---

[1] The sequence is called pseudo random because although it appears to be a random sequence it is generated using a computer algorithm.

two signals, one output signal will be the decoded bit sequence and the other output signal will be an inverted decoded bit sequence. To use the decoded signal it must be converted to an electrical signal. This occurs at a photodiode, which generates a current signal proportional to the optical power received. Now that a qualitative description of the system has been given, a mathematical analysis of it is given to describe the interference effects in the receiver.

ii. The Mathematical Model

The ideal mathematical model described here assumes no degradation in system performance and uses phasors to describe the electrical field.[2] Beginning at the laser diode and using a conventional x-y-z coordinate system, the output CW electric field, traveling in the $_+$z direction is given by:

$$\mathbf{E_{lr}(z,t)} = \mathbf{x}E_0 e^{j(\omega t - \beta z)},$$
(2.1)

where:

1. E_0 is the amplitude of the electric field in units of Volts per meter (V/m).
2. $\omega = 2\pi f$ is the angular carrier frequency of the laser and f is the emission carrier frequency of the laser. ω has units of radians per second (rad/sec), and f has units of cycles per second or Hertz (Hz).
3. $\beta = 2\pi / \lambda$ is the propagation constant of the laser. λ is the emission wavelength of the laser, β has units of 1/meter (m^{-1}), and λ has units of meters (m).
4. $\mathbf{x}$ is a unit vector in the $_+x$ direction.
5. z is the distance from the origin of the electric field in meters (m).

The output electric field is linearly polarized in the x-direction. Hence, the laser output consists of an unmodulated carrier linearly polarized in the $\mathbf{x}$ direction.

The PRBS generator creates a random sequence of 1's and 0's which is differentially encoded and then coded into an electrical signal. Figure 2.2 shows an example of a differentially coded sequence that is coded into an electrical signal. The coded sequence is 0011110101 and the bit period is 12.5 ns for a data rate of 80 Mb/s. The encoded electrical signal and the CW optical signal from the laser diode are the inputs of the phase modulator.

The phase modulator modulates the phase of the carrier wave with the information from the electrical signal, so that the input to the upper arm of the first 3-dB coupler is:

$$\mathbf{E_{1in}(z,t)} = \mathbf{E_{lr}(z,t)}e^{j\Delta\phi d(t)}$$
(2.2)

---

[2] Complex analysis is used because it makes the mathematics easier. To find the physically realizable quantity being described in a complex analysis take the real part of the waveform. As an example, the real part of (2.1) is
$\text{Re}\{\mathbf{E_{lr}(z,t)}\} = \mathbf{x}E_0 \cos(\omega t - \beta z)$.

where $\Delta\phi$ is the phase shift for a '1', and $d(t)$ is the differentially coded binary data from the PRBS generator, taking on values of 0 or 1. This equation ignores any phase shifts or loss in the fiber preceding the first 3-dB coupler.

Figure 2.2 (Electrically Coded DPSK Sequence)
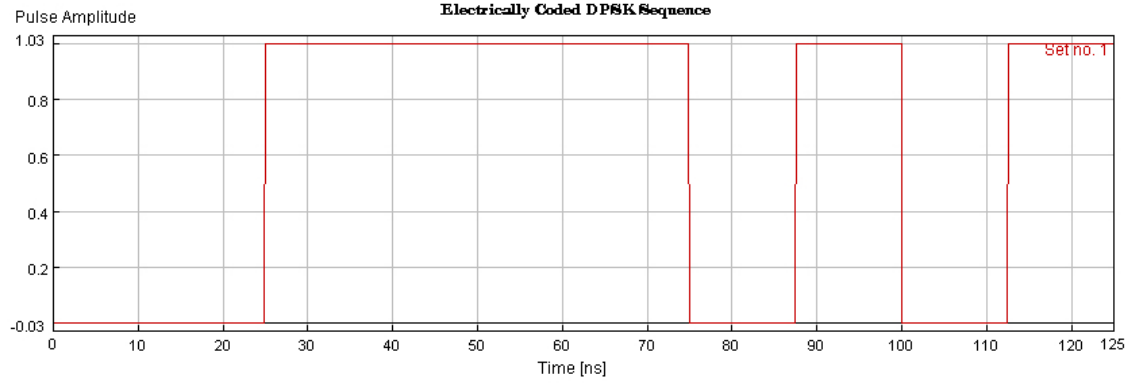
The outputs of a 3-dB coupler are described by the matrix operation:

$$\begin{bmatrix} \mathbf{E_{1out}} \\ \mathbf{E_{2out}} \end{bmatrix} = \left(\frac{1}{\sqrt{2}}\right)\begin{bmatrix} 1 & j \\ j & 1 \end{bmatrix}\begin{bmatrix} \mathbf{E_{1in}} \\ \mathbf{E_{2in}} \end{bmatrix}.$$ (2.3)

which simplifies to:

$$\begin{bmatrix} \mathbf{E_{1out}} \\ \mathbf{E_{2out}} \end{bmatrix} = \left(\frac{1}{\sqrt{2}}\right)\begin{bmatrix} \mathbf{E_{1in}} + j\mathbf{E_{2in}} \\ j\mathbf{E_{1in}} + \mathbf{E_{2in}} \end{bmatrix}.$$ (2.4)

Equation (2.4) shows that each output signal consists of a sum of the inputs, where one of the inputs is shifted by 90 degrees and where the power of both signals has been halved.[3] If $\mathbf{E_{2in}} = 0$ (second input to the coupler has no signal) then equation (2.4) becomes:

$$\begin{bmatrix} \mathbf{E_{1out3dB1}}(\mathbf{z,t}) \\ \mathbf{E_{2out3dB1}}(\mathbf{z,t}) \end{bmatrix} = (\frac{1}{\sqrt{2}})\begin{bmatrix} \mathbf{E_{1in}}(\mathbf{z,t}) \\ j\mathbf{E_{1in}}(\mathbf{z,t}) \end{bmatrix}.$$ (2.5)

Equation (2.5) shows the creation of a phase shifted reference signal.

Figure 2.1 shows that $\mathbf{E_{2out3dB1}}(\mathbf{z,t})$ continues directly to the second 3-dB coupler. However, $\mathbf{E_{1out3dB1}}$ passes through a delay line and a phase modulator before reaching the second coupler. The delay line is used to create a 1-bit delay so that a comparison may be made between adjacent bit states. The delay at the second coupler is realized by substituting $t - \tau$ for t

---

[3] The power of an optical signal is proportional to the square of the electric field. ($P \propto |E|^2$)

in $\mathbf{E_{1out3dB1}(z,t)}$ where τ is a delay equal to 1 bit period. Also, to achieve precise control over the optical phase a second phase modulator is added after the delay line. The phase modulator adds a phase of ϕ_{pm}. Hence the inputs to the second 3-dB coupler are:

$$\begin{bmatrix} \mathbf{E_{1in3dB2}} \\ \mathbf{E_{2in3dB2}} \end{bmatrix} = (\frac{1}{\sqrt{2}}) \begin{bmatrix} \mathbf{E_{1in}}(z,t-\tau)e^{j\phi_{pm}} \\ j\mathbf{E_{in}}(z,t) \end{bmatrix}. \tag{2.6}$$

Applying equation (2.4) for the second coupler yields the following output signals at this coupler:

$$\begin{bmatrix} \mathbf{E_{1out3dB2}} \\ \mathbf{E_{2out3dB2}} \end{bmatrix} = (\frac{1}{2})\mathbf{E_{lr}}(z,t) \begin{bmatrix} [e^{j(-\tau\omega+\Delta\phi d(t-\tau)+\phi_{pm})} - e^{j\Delta\phi d(t)}] \\ j[e^{j(-\tau\omega+\Delta\phi d(t-\tau)+\phi_{pm})} + e^{j\Delta\phi d(t)}] \end{bmatrix}. \tag{2.7}$$

Following the second 3-dB coupler, $\mathbf{E_{1out3dB2}}$ and $\mathbf{E_{2out3dB2}}$ are converted to electrical signals using photodiodes. The equation that relates an optical power input to an electrical current output is given by:

$$I = RP, \tag{2.8}$$

where I is the current generated by a photodiode in Amps, R is the responsivity of the photodiode in units of Amps/Watt, and P is the incident power received from an optical signal in Watts. To apply (2.8), (2.7) must be written in terms of power. Using the equation:

$$P = C|E|^2 = CEE^*, \tag{2.9}$$

where C is a constant of proportionality and E^* is the complex conjugate of E. Substituting $\mathbf{E_{1out3dB2}}$ from (2.7) into (2.9) yields:

$$P_1 = \left(\frac{P_0}{4}\right)\sigma\sigma^*, \tag{2.10}$$

where

$$P_0 = CE_0^2, \tag{2.11}$$

and

$$\sigma = e^{j(-\tau\omega+\Delta\phi d(t-\tau)+\phi_{pm})} - e^{j\Delta\phi d(t)}. \tag{2.12}$$

Hence, the power at the upper output of the second coupler is:

$$P_1 = \left(\frac{P_0}{4}\right)[e^{j(-\tau\omega+\Delta\phi d(t-\tau)+\phi_{pm})} - e^{j\Delta\phi d(t)}][e^{-j(-\tau\omega+\Delta\phi d(t-\tau)+\phi_{pm})} - e^{-j\Delta\phi d(t)}].$$ (2.13)

Rearranging,

$$P_1 = \left(\frac{P_0}{4}\right)[2 - e^{j(-\tau\omega+\Delta\phi d(t-\tau)-\Delta\phi d(t)+\phi_{pm})} - e^{-j(-\tau\omega+\Delta\phi d(t-\tau)-\Delta\phi d(t)+\phi_{pm})}]$$ (2.14)

which simplifies to

$$\boxed{P_1 = \left(\frac{P_0}{2}\right)[1 - \cos(\Delta\phi d(t-\tau) - \Delta\phi d(t) + \phi_{pm} - \tau\omega)]}$$ (2.15)

Repeating for $\mathbf{E_{2out3dB2}}$ yields:

$$\boxed{P_2 = \left(\frac{P_0}{2}\right)[1 + \cos(\Delta\phi d(t-\tau) - \Delta\phi d(t) + \phi_{pm} - \tau\omega)]}$$ (2.16)

for the lower output. If the phase modulator in the delay arm is driven such that $\phi_{pm} - \tau\omega = 2\pi n$, where n is an integer. Then (2.15) and (2.16) simplify to:

$$\boxed{P_1 = \left(\frac{P_0}{2}\right)[1 - \cos(\Delta\phi d(t-\tau) - \Delta\phi d(t)]}$$ (2.17)

$$\boxed{P_2 = \left(\frac{P_0}{2}\right)[1 + \cos(\Delta\phi d(t-\tau) - \Delta\phi d(t)]}.$$ (2.18)

Now applying (2.8) to (2.17) and (2.18) to find the electric currents produced by the photodiode the final signal currents are obtained:

$$\begin{bmatrix} I_1 \\ I_2 \end{bmatrix} = \left(\frac{RP_0}{2}\right)\begin{bmatrix} (1 - \cos(\Delta\phi d(t-\tau) - \Delta\phi d(t))) \\ (1 + \cos(\Delta\phi d(t-\tau) - \Delta\phi d(t))) \end{bmatrix}.$$ (2.19)

Figure 2.3 shows an example of how this communication system should work. A random 20 bit sequence is transmitted at 80 Mb/s in figure 2.3a and then differentially encoded in figure 2.3b. Figures 2.3c and 2.3d show the outputs of the second coupler after (2.17) and (2.18) are applied with $P_0 = 1$ mW, $\Delta\phi = \pi$, $\tau = 12.5$ ns (1 bit delay). The phase modulator in the receiver is driven such that $\phi_{pm} - \tau\omega = 2\pi n$. Figures 2.3e and figure 2.3f illustrate the output of the photodiodes when $R = 1$ A/W. As proof that the receiver has decoded the input sequence, figure 2.3e, the

output waveform of the upper arm photodiode output is identical to the input bit stream. Figure 2.3f shows an inverted version of the input waveform.
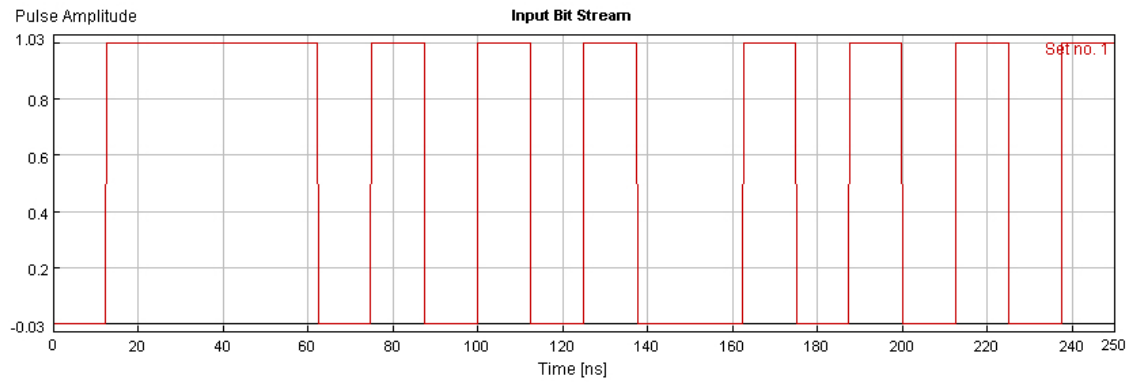
Figure 2.3a (Input Bit Stream)

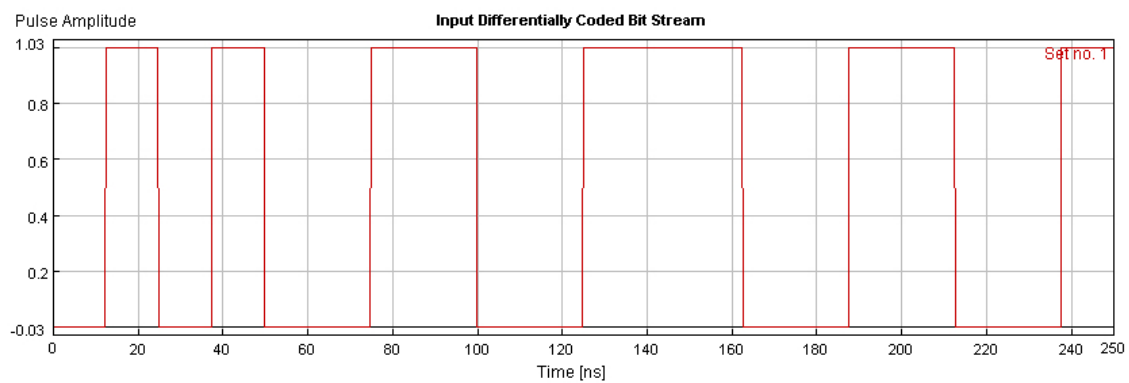Figure 2.3b (Differentially Coded Input Bit Stream)
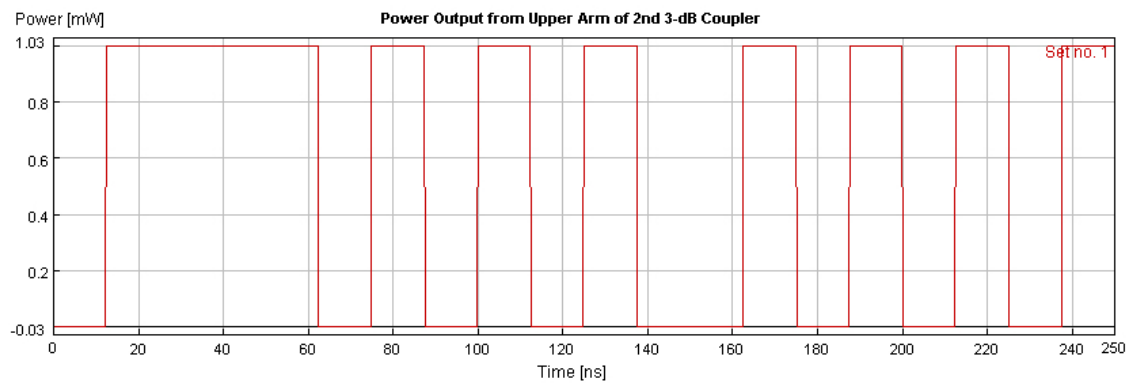

Figure 2.3c (Illustration of Equation 2.17)
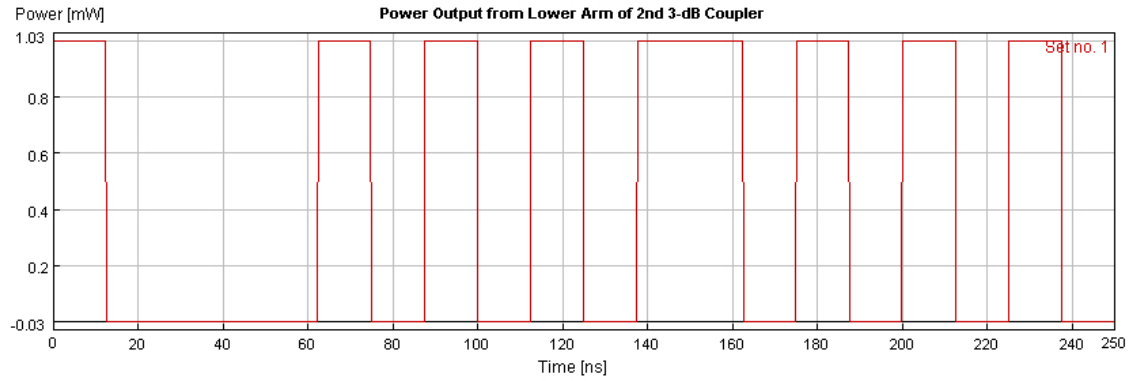

Figure 2.3d (Illustration of Equation 2.18)
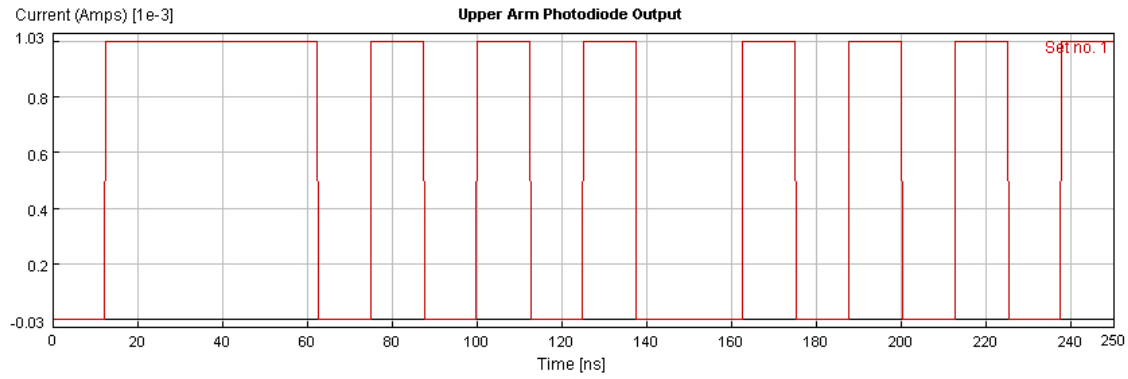
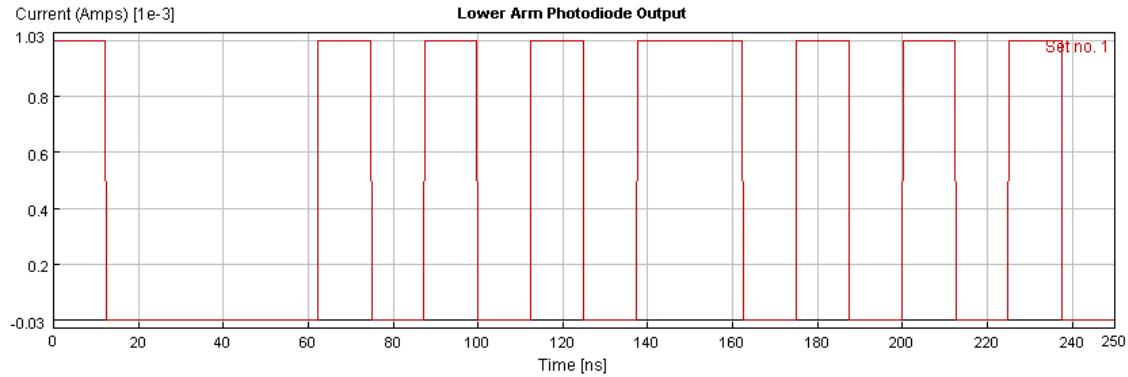Figure 2.3e (Illustration of Upper Arm Photodiode Output)

Figure2.3f (Illustration of Lower Arm Photodiode Output)

B. Advantages of this Communication System

In a typical coherent system, another laser, known as a local oscillator (LO) is encountered at the receiver. The LO creates the reference signal that is produced in this design using a coupler. Receivers are classified as either homodyne or heterodyne when a LO is used. If the emission frequency of the LO is the same as the emission frequency of the transmitter laser, the receiver is homodyne. If the emission frequencies are different then it is a heterodyne receiver. Prior research in optical communications revealed that homodyne receivers have a 3-dB improvement in receiver sensitivity over heterodyne receivers. [10] This means that a homodyne receiver can accurately detect weaker received signals. Additionally, a heterodyne

receiver generates an intermediate frequency signal component that needs to be extracted with a band pass filter. Hence, a heterodyne receiver is more complex. The disadvantage of a homodyne system is that optical phase and frequency requirements are more stringent. Phase stability is needed to enable interference effects discussed in section II, part A. Frequency stability is required so that the transmitting laser and the LO do not generate an intermediate frequency. In this design, the frequency stability is less relevant since the transmitter creates its own reference signal.

Much prior research [4], [11]-[13] has required a significant amount of post-detection signal processing. The design of the receiver in this paper avoids this, using only a photodiode. This keeps the design simple. Others have tried to do this, with some success. [11] However, a LO was used and there was a significant amount of post-detection electrical processing. An interferometer in [14] used beam splitting mirrors, which caused an additional 3 dB loss in signal power. Using directional couplers avoids this excessive amount of loss.

III. Computer Simulation

       The mathematics of this communication system are complicated when system performance is degraded by noise, dispersion, or losses, so a computer simulation program is employed to model this system. In using this simulation program various system parameters can be varied and results can be obtained relatively quickly. However, in order to use this simulation it is necessary to understand how it models the system.

       The simulation program used to model the system is VPITransmissionMaker made by Virtual Photonics Incorporated (VPI). This program uses a graphical user interface (GUI) to model different types of optical communication systems. The different components for the receiver proposed in this paper are depicted as block modules in the simulation program. The user connects the inputs and outputs of the modules appropriately to model the system being designed. Various parameters for each module are set before simulating the system. Figure 2.1 shows a block diagram of the system created in VPITransmissionMaker.

       Since this is a computer program, the waveforms generated are discretely sampled waveforms. Recall that equation 2.1 is the waveform for the output of a laser diode. To determine the value of the waveform at a specific time in the simulation the user will specify a sample rate for this waveform and at equal time intervals the waveform will be sampled, creating an array of samples that represents the waveform values at different times.

       VPITransmissionMaker offers several different ways to process information in simulations. The principal way that information is processed in the simulation is in block mode. In block mode, all samples entering a module will be processed in that module before any sample is passed to the next module. As an example, in the case of the laser diode connecting to the phase modulator output, all of the samples representing the output of the laser diode are generated before the first sample is passed to the phase modulator. Hence, no two modules are operating at the same time.

.

IV. System Evaluation

A. BER Approximation Method

      Section II described an ideal simulation where the output waveform was identical to the input bit sequence. In practice, no communication system operates ideally and there must be a certain amount of tolerance for error. As shown in figure 4.1, the transmitted bit sequence can be distorted at the receiver output due to non-ideal behavior of the system. If the distortion is severe enough the receiver may misinterpret information, causing errors.   Since this is a digital system an error occurs whenever a transmitted '1' is interpreted as a '0' at the receiver (and vice versa).

      The frequency of errors in a digital communication system is specified by the bit error ratio (BER). The BER is the number of errors occurring in a system given a certain number of bits transmitted. For instance, a BER of 10^{-9}, the standard required of optical communication systems means that 1 out of 10^9 bits will be in error.

      To determine that a BER of a system is 10^{-9} requires that at least 10^9 bits are simulated. However, the amount of time it takes for simulation of 10^9 bits is exorbitant. To obtain a BER value simulating only a relatively small number of bits a commonly used statistical approximation method is used.

Figure 4.1a (Coded Bit Stream from Pulse Generator)

Figure 4.1b (Received Electrical Signal)

The method is a Gaussian approximation [14] given by:

$$BER = \frac{n_1}{2(n_0 + n_1)} erfc(\frac{|\mu_1 - D|}{\sqrt{2}\sigma_1}) + \frac{n_0}{2(n_0 + n_1)} erfc(\frac{|\mu_0 - D|}{\sqrt{2}\sigma_0}).$$ (4.1)

In this equation,

n_1 = the number of 1's transmitted,

n_0 = the number of 0's transmitted,

μ_1 = the mean current in a '1',

μ_0 = the mean current in a '0',

σ_1 = the standard deviation of a '1',

σ_0 = the standard deviation of a '0',

D = decision threshold for 1's and 0's,

and the complimentary error function is defined as:

$$erfc(x) = \frac{2}{\sqrt{\pi}} \int_x^{\infty} e^{-y^2} dy.$$ (4.2)

If 1's and 0's are transmitted with equal probability the equation for BER becomes:

$$BER \approx \frac{1}{\sqrt{2\pi}} \frac{e^{-Q^2/2}}{Q},$$ (4.3)

where

$$Q = \frac{|\mu_1 - \mu_0|}{\sigma_1 + \sigma_0}.$$ (4.4)

Q is related to the signal to noise ratio. Note that in (4.4) the numerator is proportional to the optical signal and the denominator is proportional to photodiode noise. A value of $Q \approx 6$ corresponds to a 10^{-9} BER. As Q increases the BER improves. Unless otherwise noted, the simulated bit sequences consists of 1's and 0's transmitted with equal probability so that (4.3) and (4.4) apply. The BER approximation method shown here provides a straightforward method to determine the BER in simulations. It will be shown in section VI that this technique can also be applied to a hardware model to obtain a BER estimate.

B. Obtaining Accurate Results

In the simulator, accurate estimates of the BER depend on the sample rate and the number of bits simulated. The sample rate determines the simulation bandwidth, which is one half of the sample rate. The higher the bandwidth, the more accurate the simulation. Additionally, the greater the number of bits simulated, the greater the accuracy of the BER

calculation. Ideally, the sample rate and number of bits simulated should be as high as possible. However, for computational speed and efficiency both the number of bits and the sample rate need to be restricted. There is a concern in doing this, if the sample rate is too low or there are not enough bits simulated then BER values for the same simulation will not be the same for different random bit sequences. To obtain a reasonably accurate BER, multiple simulations were run with different random bit sequences to determine when BER values obtained began to converge. In determining convergence it is the Q value which needs examination. [15] As shown in (4.3) the BER is computed from the Q value. Equation (4.3) is a non-linear equation so averaging BER values from multiple simulations cannot be used to determine convergence.

Table (4.1 BER Convergence based on Q values)

Number of bits Sumulated	2048		4096	
Sample Rate (GHz)	5.12		5.12	
Trial Number	Q	BER	Q	BER
1	6.387503	$8.628*10^{-11}$	6.122233	$4.731*10^{-10}$
2	5.947898	$1.395*10^{-9}$	6.369016	$9.736*10^{-11}$
3	6.006021	$9.757*10^{-10}$	6.128475	$4.549*10^{-10}$
4	6.578136	$2.435*10^{-11}$	6.072542	$6.458*10^{-10}$
5	6.311661	$1.413*10^{-10}$	6.33885	$1.185*10^{-10}$
6	6.155796	$3.830*10^{-10}$	6.107432	$5.192*10^{-10}$
Mean Values	6.231169	$2.372*10^{-10}$	6.189758	$3.088*10^{-10}$
Standard Deviation	0.239967		0.128992	

Table 4.1 shows simulation results where six different bit sequences were tried with 2048 and 4096 bits being simulated. Even though the mean BER values[1] were similar, simulating 4096 gave a lower standard deviation value for Q. When 2048 bits were simulated the BER was generally accurate to within two orders of magnitude, when 4096 bit were simulated the BER was generally accurate to within one order of magnitude. Since the BER method being used is only an estimate, being accurate to one order of magnitude will suffice. It gives both a reasonable BER estimate and computational efficiency. Thus, unless otherwise specified all simulations use 4096 bits at a sample rate of 5.12 Gsamples/second.

---

[1] The mean BER value in this table is computed from the mean Q value, not by averaging the BER from the six trials.

V. Non-Ideal Behavior

Thus far, the qualitative and quantitative descriptions of this system have ignored effects that degrade performance. To model and design a practical system, the simulator accounts for such effects by using typical specifications for real components. Unless otherwise specified, the simulations in this section model a system operating at an 80 Mb/s data rate. To focus on the optical receiver characteristics, the communication channel in Figure 2.1 is ignored by setting the fiber length to 0 km.

A. Transmitter Characteristics

The transmitter has three components, a laser light source, an electric pulse generator used to generate data, and a phase modulator that converts the electrical signal to optical phase modulation.

i. Laser Characteristics

The main laser characteristic that degrades a coherent optical system is the laser linewidth. In the ideal simulation the linewidth is ignored and the laser emits light at a single frequency. A real laser emits light over a range of frequencies. Linewidth is a measure of this range. Coherent optical communication systems require a narrow laser linewidth because the phase of the optical wave carries the signal, not the amplitude. Thus obtaining an accurate description of the laser linewidth is necessary to accurately characterize the system.

To understand the various noise sources in a laser diode it is important to have a basic understanding of how a laser diode works. A laser diode consists of two semiconductor materials, one of p-type and one of n-type, that are connected to form a p-n junction. At the junction there is a region known as the active layer. It is in this region that the lasing process takes place. In the active layer, there are positive (hole) and negative (electron) charge carriers that are allowed to assume one of two possible energy levels, the valence band or the conduction band. Charge carriers in the conduction band are at a higher energy level than those in the valence band. When a charge carrier transitions from the conduction band to the valence band, the charge carrier must lose energy to assume the lower energy level of the valence band. This release of energy occurs through the creation of a photon of light at a specific frequency. Conversely, during a transition from the valence band to the conduction band, energy must be added (absorption of a photon) to a charge carrier in order for it to assume the higher energy state in the conduction band.

Under thermal equilibrium conditions most charge carriers reside in the valence band. In thermal equilibrium three random processes will take place. One of these processes is the absorption process, where a charge carrier in the valence band may absorb a photon, entering the conduction band. Another is spontaneous emission, whereby a charge carrier in the conduction band will randomly transition to the valence band with the emission of a photon. Finally, in a third process known as stimulated emission, a photon encountering a charge carrier in the conduction band stimulates the charge carrier to release a photon and return to the valence band. The emitted photon has the same frequency and phase as the photon stimulating this transition.

It is this third process which allows the lasing process to begin. The stimulated emission of a charge carrier results in two photons which in turn can cause other stimulated emissions. If this process is repeated, many photons of the same phase and frequency are created. In thermal equilibrium most charge carriers are in the valence state. By achieving population inversion,

most charge carriers are in the conduction band and the stimulated emission process dominates, creating a CW beam of photons all having the same frequency and phase. To achieve population inversion an electric field is applied across the junction. The source of the electric field is an external voltage source connected to the semiconductor material. In order for population inversion to exist the electric field must be of sufficient strength. The minimum current from the voltage source that will create the required electric field is the threshold current. To further enhance the effect of stimulated emission a gain medium is created. At both ends of the active region two reflective materials are placed to reflect incident photons back and forth in the active region. Some of these photons do not reflect and are transmitted through the reflective material to produce the output laser light beam. Those that are reflected bounce back and continue to induce stimulated emissions.

While in theory stimulated emission generates photons all having the same frequency, it has been shown that a laser cavity can also support resonant frequencies, occurring at equal frequency intervals. Contributions to the linewidth from resonant frequencies potentially can corrupt a signal. The Side Mode Suppression ratio (SMS) measures the ability of a laser to suppress resonant frequencies. It is a ratio of the power density in the dominant frequency to the highest power density achieved in a resonant frequency. In a hardware setup of this system two distributed feedback (DFB) lasers will be used which have SMS values exceeding 30 dB so the presence of side modes is not an issue in this system.

Within the main lasing mode there are noise mechanisms that can broaden the spectral output of a laser. The dominant mechanism is phase noise which is due primarily to spontaneous emission (described above) and random fluctuations in the number of charge carriers. [16] To represent phase noise, a phase term, $\int \omega(\tau)d\tau$ is added to (2.1) so that the laser output becomes:

$$\mathbf{E_{lr}(z,t)} = \mathbf{x}E_0 e^{j(\omega t - \beta z + \int \omega(\tau)d\tau)} \tag{5.1}$$

and the frequency of the light is a function of time. The added phase term, $\int \omega(\tau)d\tau$ represents the accumulated phase of a white noise process.[1] The variance of the phase noise is:

$$\sigma_{pn}^2 = 2\pi\Delta f \tag{5.2}$$

where Δf is the linewidth in Hertz. Figure 5.1 shows the effect of phase noise on the spectral output of a laser.

---

[1] See appendix B for the definition of a white noise process.

Figure 5.1.a (Source at 229 THz with 0 Linewidth)
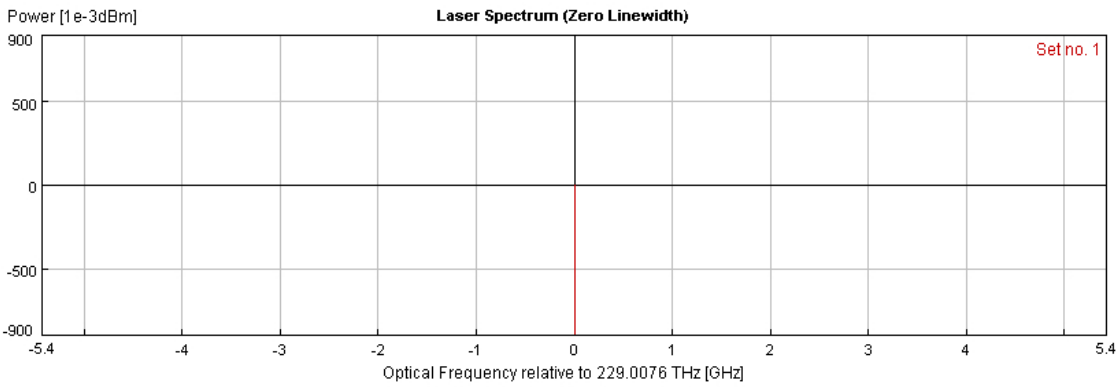
Figure 5.1.b (Source at 229 Thz with 5 Mhz Linewidth)
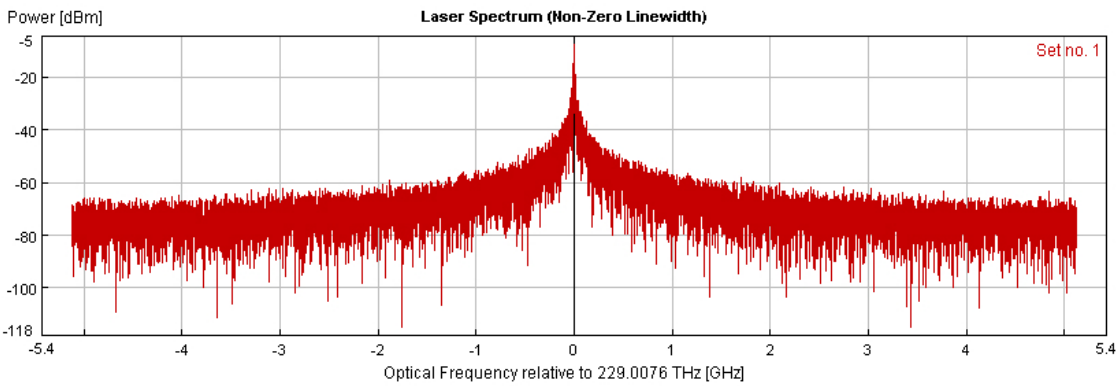
The two DFB lasers being used to test this communication system have different linewidth characteristics. One laser has a linewidth of only 3 kHz while the exact linewidth of the other laser is unknown, but estimated to be in the range from 1-10 MHz (typical for this type of laser). Figure 5.2 shows simulation results investigating the effect of linewidth on BER at 80 Mb/s. It is evident from this figure that system performance relies heavily on the linewidth. From this plot the approximate linewidth where the BER is 10^{-9} is approximately 3.136 MHz, so to achieve a 10^{-9} BER the linewidth of the laser being used must be less than 3.136 MHz. Figure 5.3 shows a received bit sequence at a BER of 10^{-9}. Figure 5.4 shows a group of waterfall plots of BER vs. linewidth for other data rates. It is seen that as the data rate increases the linewidth requirements needed to achieve a 10^{-9} BER are relaxed.

21

Figure 5.2 (BER vs. Linewidth at 80 Mb/s)
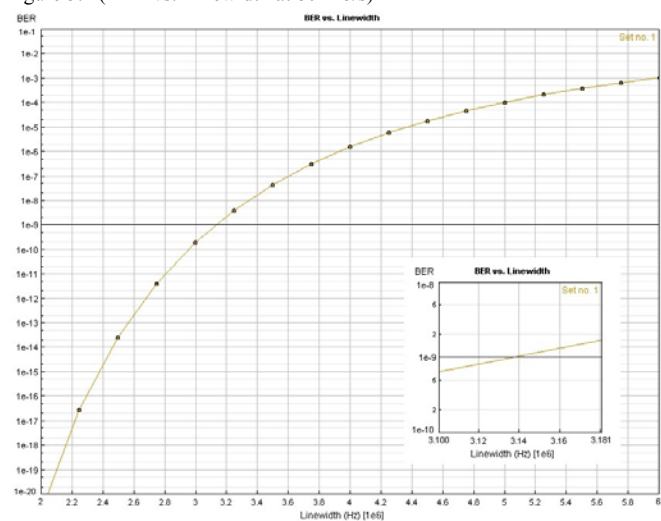
Figure 5.3 (Received Bit Sequence Corresponding to a 10^{-9} BER)
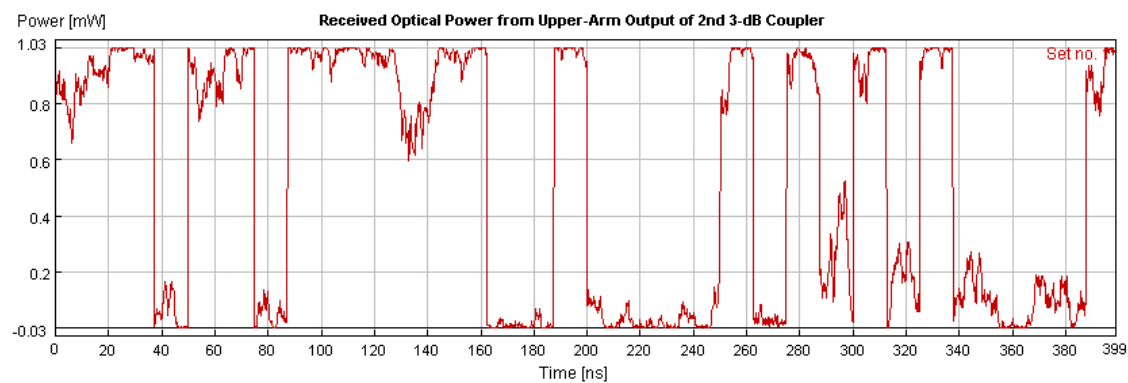
Figure 5.4 (BER vs. Linewidth Plots at Different Data Rates)
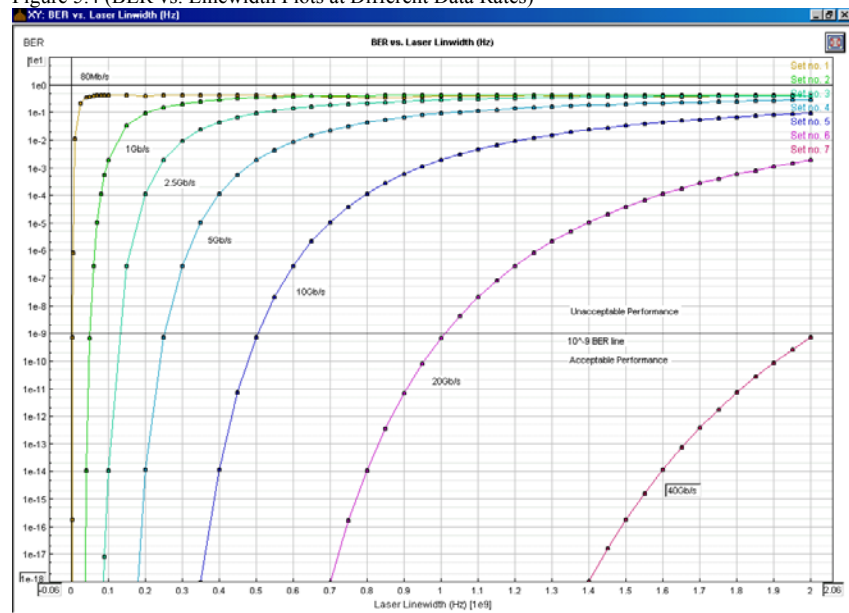
ii. Pulse Generator Characteristics

The ideal simulation assumes that the current level of the electrical waveform instantaneously transitions from 1 to 0 or from 0 to 1 (see figure 5.5a). A pulse generator in a real system is band-limited, giving each pulse a finite transition time known as the rise time, t_r. This results in a rounded pulse shape (see figure 5.5b). Formally, the rise time is defined as the time it takes for the amplitude of a signal to vary between 10% and 90% of its final value. To account for a rise time, the square pulses emitted from the pulse generator undergo an impulse response $h(t)$, such that $y(t) = x(t) * h(t)$ where $x(t)$ is the input square pulse train, $y(t)$ is the output rounded pulses, and $h(t) = \dfrac{2}{\sqrt{\pi T}} e^{-(2t/T)^2}$ is the impulse response of the pulse where, T is the $1/e$ pulse duration and $*$ indicates the mathematical convolution operation.

Figure 5.5.a (Un-Rounded Pulse)
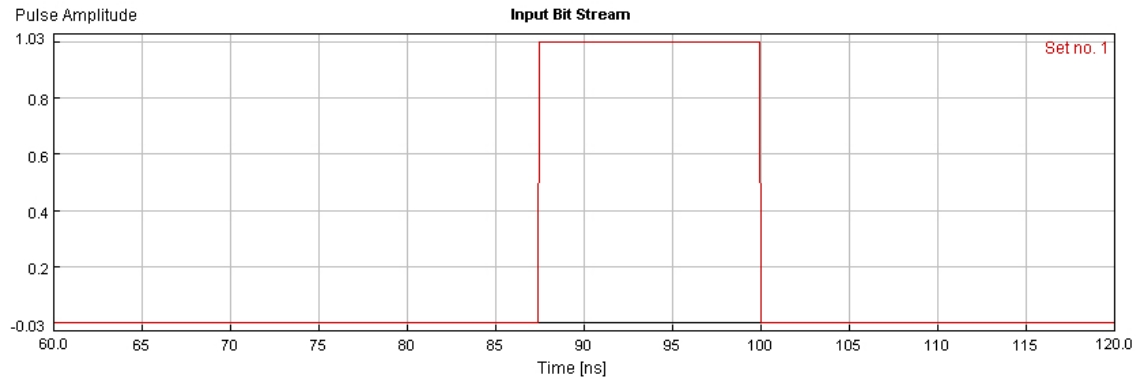
Figure 5.5.b (Rounded Pulse)
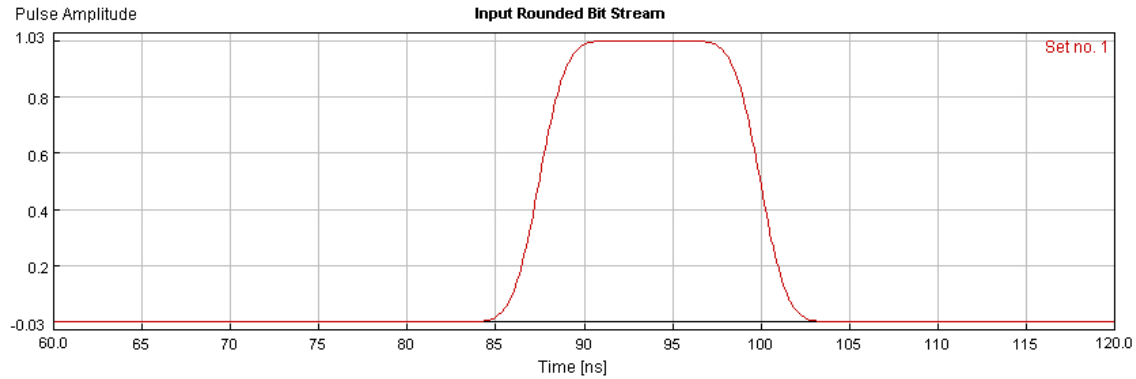
In a hardware setup an Agilent 81104A programmable pulse generator will be used to generate the bit stream. Its rise time can be set in the range of 3 ns to 200 ms, depending on the bit rate. Figure 5.6 depicts the simulation results due to rise time, assuming a laser with negligible linewidth is used. From figure 5.6 it is clear that the rise time does not significantly impact BER until around 13 ns, a time much greater than the 3 ns rise time possible by the pulse generator and larger than the bit period of 12.5 ns.

Figure 5.6 (Effect of Rise Time on BER at 80 Mb/s)
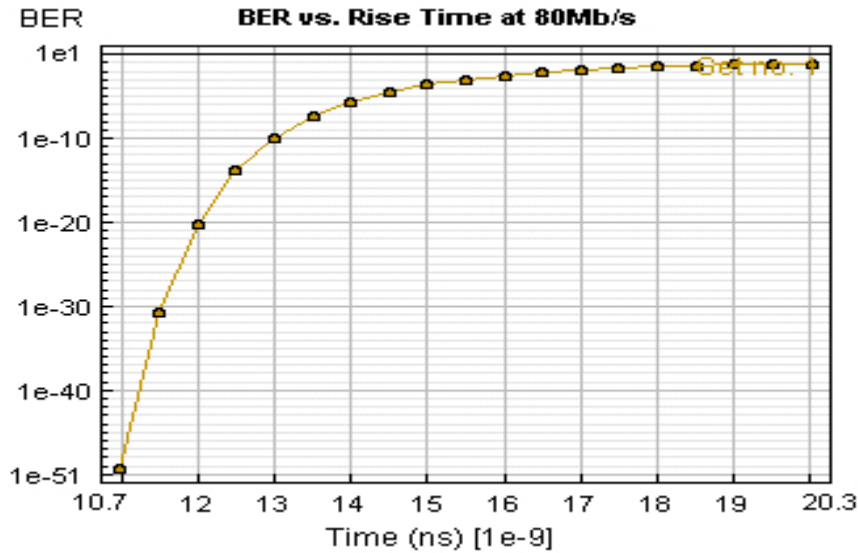
B. Channel Effects

To focus on receiver characterization in the simulations, the fiber channel length was assumed to be 0 km so that the transmitter connects directly to the receiver, ignoring channel effects. In a real system channel effects are important. Two primary effects degrade a signal upon propagation in a fiber, dispersion and attenuation. Dispersion and attenuation of optical fiber have no significant effects in this system.

Dispersion must be taken into account to analyze the actual performance limits of this receiver in the presence of a channel. Dispersion is the spreading of a pulse in time as it propagates along the fiber.[2] With too much dispersion, energy spreads to adjacent pulses, corrupting the data stream. At 1310 nm, dispersion is small, which is why this emission wavelength is being used.

Fiber attenuation is the decay of signal energy as it propagates through an optical fiber. It is expressed as loss in dB/km. Attenuation primarily occurs because some of the light is scattered by impurities within the fiber. It is an important issue in long channels where a significant amount of signal loss may occur, decreasing the received optical power (discussed in section V part C) and degrading receiver performance.

Aside from the effects of dispersion and attenuation, the other effects that degrade a signal in optical fibers are nonlinear. Such effects become important when the laser diode power output is high. For emitted power less than 1 mW nonlinear effects are ignored. Since the laser diode output power in the hardware setup is around 1 mW nonlinear effects are ignored in simulations.

---

[2] For an in depth description of dispersion see appendix B

C. Receiver Effects

To make the optical signal useful the signal must be converted back to an electrical signal. This conversion process takes place on a photodiode within the receiver. The optical power incident on the photodiode creates an electrical current proportional to the incident optical power. Two types of photodiodes can be used in an optical receiver, a P-type Intrinsic N-type (PIN) photodiode or an Avalanche Photodiode (APD). In this receiver, an InGaAs PIN photodiode will be used.

i. Photodiode Noise

Signal current is not the only current present in a photodiode. Photodiodes inherently have noise currents which can corrupt the signal current. To prevent photodiode noise from significantly affecting system performance the signal to noise ratio of the system needs to be above a critical level. Assuming the laser linewidth is narrow enough to prevent degradation from phase noise, photodiode noise can still be significant when the received optical power (ROP) is sufficiently low. ROP depends on the laser output power and system losses. System losses can take place in the channel as discussed in section V part B and in system components such as the phase modulator and couplers.

Receiver noise degrades the system by reducing receiver sensitivity. As the ROP decreases, it becomes increasingly difficult to distinguish the signal current from noise current. Eventually, if the signal current is too small, it cannot be distinguished from the noise current. Since the goal of this communication system is to transmit and receive with a BER of 10^{-9} or better, receiver sensitivity is defined as the required ROP needed to obtain a 10^{-9} BER.

The received optical signal generates a current i_s. In the presence of noise, the total current, i_Σ emerging from a photodiode, consists of a signal current i_s, and noise currents i_n.

$$i_\Sigma = i_s + i_n . \tag{5.3}$$

The variance in the noise current consists of the sum of several current components. The primary noises in the photodiode are the dark current $\langle i_d^2 \rangle$, shot noise current $\langle i_Q^2 \rangle$, and thermal noise current $\langle i_T^2 \rangle$. The sum of these three currents leads to an expression for the variance of the total noise current:

$$\langle i_n^2 \rangle = \langle i_d^2 \rangle + \langle i_Q^2 \rangle + \langle i_T^2 \rangle . \tag{5.4}$$

The simulation uses commonly accepted formulas [14], [17], [18] to calculate the contribution of each current component.

The dark current through a photodiode is present when no light is incident on the photodiode. It is usually the smallest of the three noise currents. Shot noise is a measure of the randomness of the photo-detection process. Shot noise is usually specified by its Power Spectral Density, (PSD). The PSD in $A/\sqrt{Hz}$ for the shot noise current is given by:

$$N_{sh} = \sqrt{2q(i_s + i_d)} \tag{5.5}$$

where $q = 1.60 \cdot 10^{-19}$ Coulombs (C) is the electron charge. Generally shot noise is greater than dark current. Thermal noise accounts for a temperature dependent noise current in the photodiode. It often has the most significant effect on system performance, with a PSD of

$$N_T = \sqrt{\frac{4k_bT}{R_L}}$$ (5.6)

where $k_b = 1.38 * 10^{-23}$ J/K is Boltzman's constant, R_L (Ω) is a load resistor for the photodiode, and T is the temperature in degrees Kelvin.

ii. Photodiode Bandwidth
In addition to noise another consideration that needs examination within a photodiode is its bandwidth. The bandwidth of the photodiode determines its rise time of the photodiode and the maximum data rate it can process. InGaAs PIN photodiodes typically have bandwidths in the GHz range so at a transmission rate of 80 Mb/s, bandwidth is not an issue for this system. However, at high data rates this is an important system consideration.

iii. Simulation Parameters
Simulations used to determine receiver sensitivity used the photodiode characteristics shown in table 5.2. These characteristics are based on the InGaAs photodiode used in the hardware system. As discussed in section IV, the simulation bandwidth is only 2.56 GHz which is less than the 3-dB photodiode bandwidth of 6 GHz. However, because the data rate of the system is only 80 Mb/s only a small portion of the 2.56 GHz bandwidth is utilized so simulating the system with a bandwidth less than the photodiode bandwidth does not significantly affect results.

Table 5.2 (InGaAs Photodiode Parameters used in Computer Simulations)

Responsivity	.33 A/W
3-dB Electrical Bandwidth	6 GHz
Dark Current max (typical)	15 nA
Thermal Noise Current	18.2 $pA/\sqrt{Hz}$
Shot Noise PSD	$2q(i_s + i_d)$ $A/\sqrt{Hz}$

Figure 5.7 (BER vs. Received Optical Power in the Presence of Receiver Noise at 80 Mb/s)
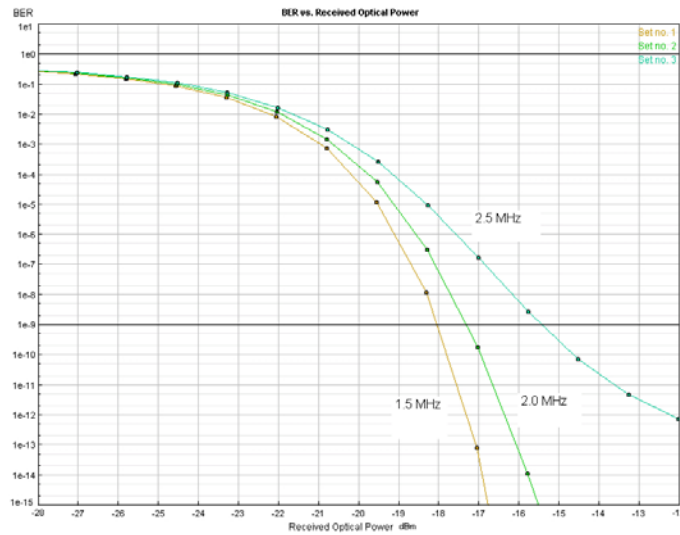
Table 5.3 (Received Optical Power vs. Linewidth in the Presence of Receiver Noise)

Linewidth (MHz)	ROP (μW)
1.5	15.7
2.0	18.53
2.5	28.61

Figure 5.7 shows simulation results where the effect of ROP on BER was explored at different linewidths using the photodiode parameters of table 5.2. Recall that in the noise-free infinite bandwidth system 3.136 MHz was the maximum permissible linewidth to achieve a 10^{-9} BER. In the simulation results shown in figure 5.7 the linewidths simulated were chosen to be less than this to reveal how changing the linewidth affected the required received optical power. Table 5.3 contains data showing the ROP required at different linewidths obtained from figure 5.7. This table shows that increasing the laser linewidth causes the required ROP to increase and hence reduces receiver sensitivity.

iv. Polarization

In the second coupler, interference takes place between the electric fields to recover the input bit stream. In section II it was assumed that the two signals in (2.7) have the same state of polarization (SOP) so that maximum interference takes place. However, in a real system the signals may not have the same SOP due to fiber or component effects. If a polarization mismatch exists only the components of the electric field lying in the same polarization will interfere.

Figure 5.8 shows the effects of a polarization mismatch on BER in a simulation. The laser linewidth of the laser is 1.5 MHz, the ROP at the photodiodes is 100 μW and the receiver characteristics of table 5.2 are used. The polarization of the signal propagating in the lower arm in figure 2.1 has been changed with respect to the polarization of the signal in the upper arm. The BER is highest at 90 degrees where the SOPs of the two signals are perpendicular to one another so that no interference takes place between the two signals. Figure 5.9 shows how having different SOPs effects the BER. Comparing figures 5.9a and 5.9b shows that the difference in current levels between a '1' and '0' is reduced, decreasing the contrast of the signal.

This is analogous to reducing the ROP. If the polarizations differ by 90 degrees then no interference occurs and the signal disappears as in figure 5.9c. If the polarizations mismatch by 180 degrees then the output signal is inverted as shown in figure 5.9d.

Figure 5.8 (BER vs. Angular Difference in State of Polarization Directions)
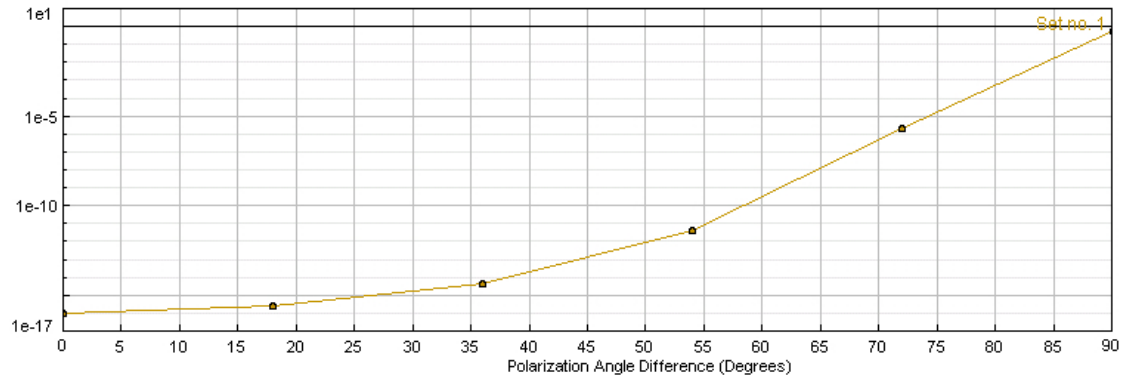
Figure 5.9a (Output Bit Sequence at a Relative Angle of 0 Degrees)
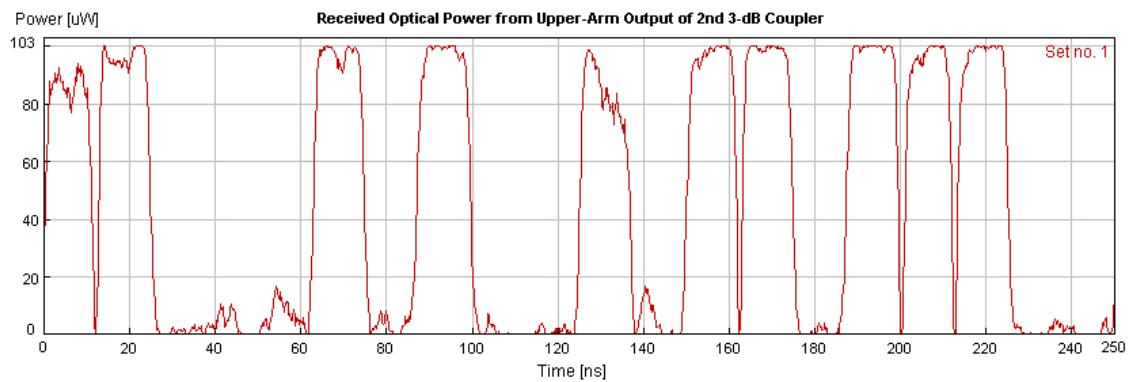
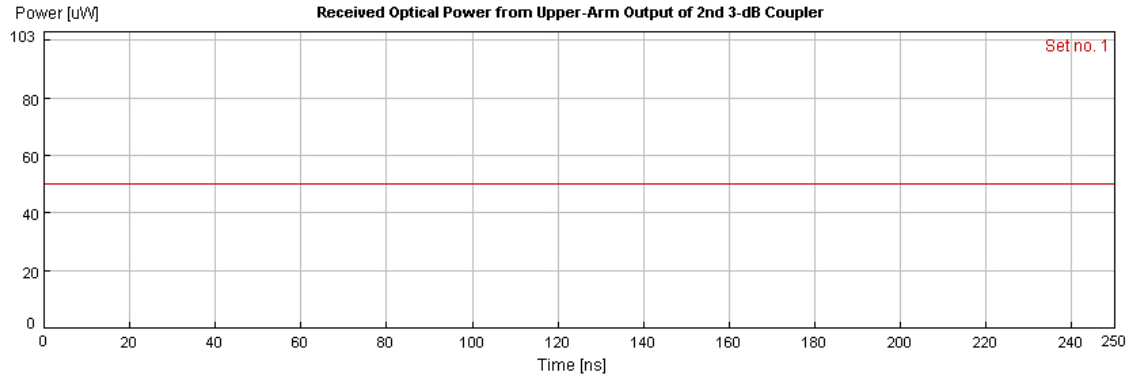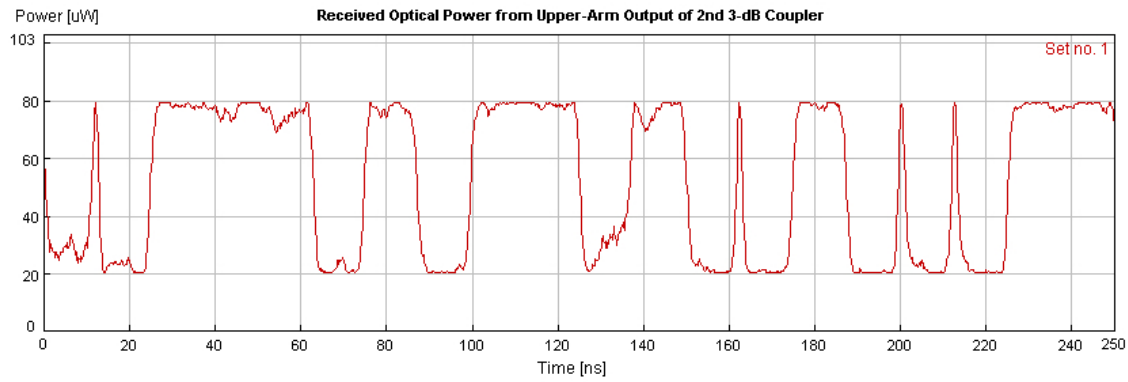Figure 5.9b (Output Bit Sequence at a Relative Angle of 72 Degrees)
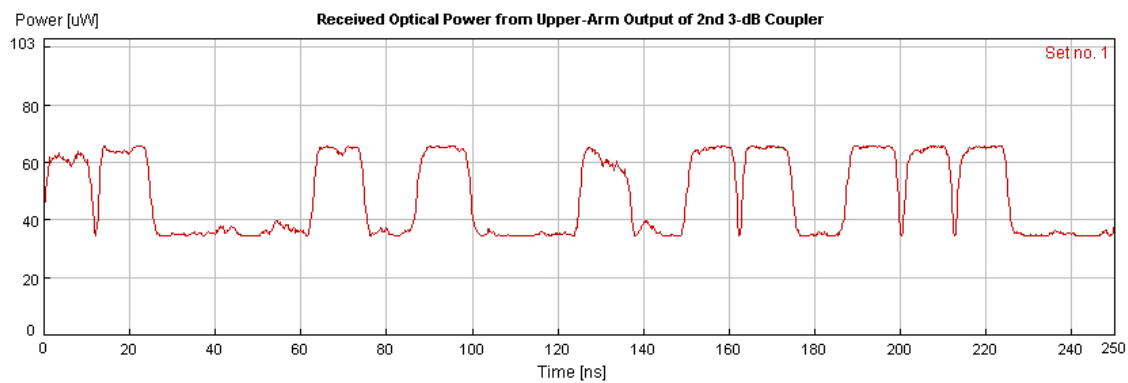
Figure 5.9c (Output Bit Sequence at a Relative Angle of 90 Degrees)

Figure 5.9d (Output Bit Sequence at a Relative Angle of 126 Degrees)

v. The Effects of an Improper Phase Shift

Here, the effect of an improper phase shift, ϕ_{PM} will be investigated. Figure 5.10 shows simulation results of an imprecise phase shift at 80 Mb/s. The linewidth for this simulation is 1.5 MHz, the ROP is 100 μW, and the photodiode has the characteristics of Table 5.2. At 80 Mb/s a -153 degree phase shift satisfies the $\phi_{PM} - \tau\omega = 2\pi\pi$ condition. It is at this phase shift value that the BER is minimized. In the range from −140 to −166 degrees the BER meets receiver requirements of a 10^{-9} BER or better. Figure 5.11 shows the appearance of bit streams at the output of the second coupler at different phase shift values. Figure 5.11a is the input bit stream. Figures 5.11c-5.11e show distorted outputs at improper phase shifts. Figure 5.11f shows that at a 57 degree phase shift the bit stream is inverted.

Figure 5.10 (Investigation of Improper Phase Shift on BER)
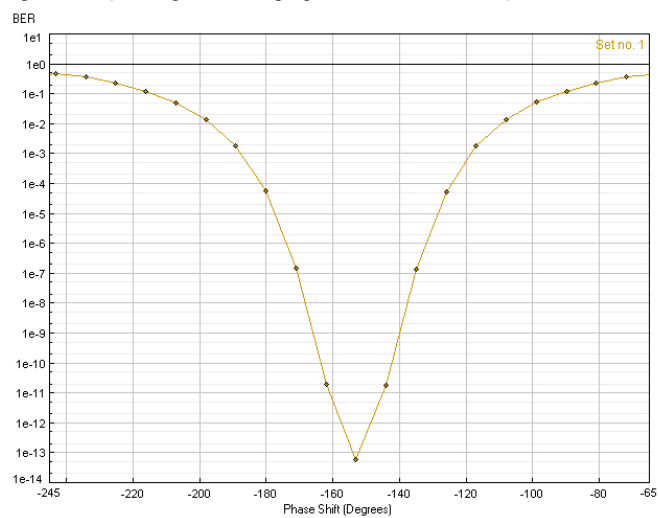
Figure 5.11a (Input Bit Stream)
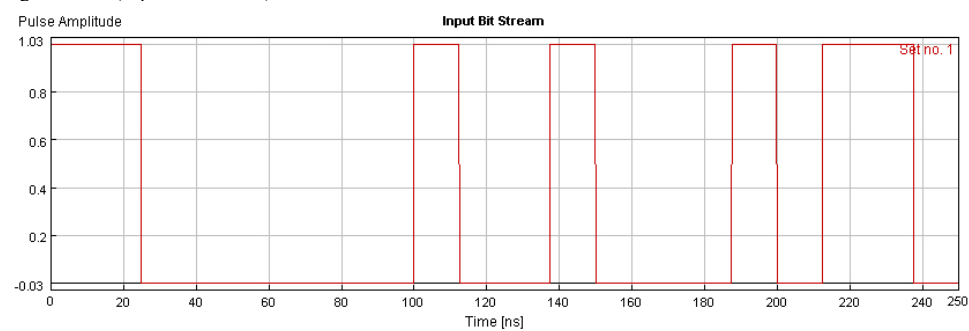
Figure 5.11b (-153 Degree Phase Shift)

Figure 5.11c (-198 Degree Phase Shift)

Figure 5.11d (-225 Degree Phase Shift)
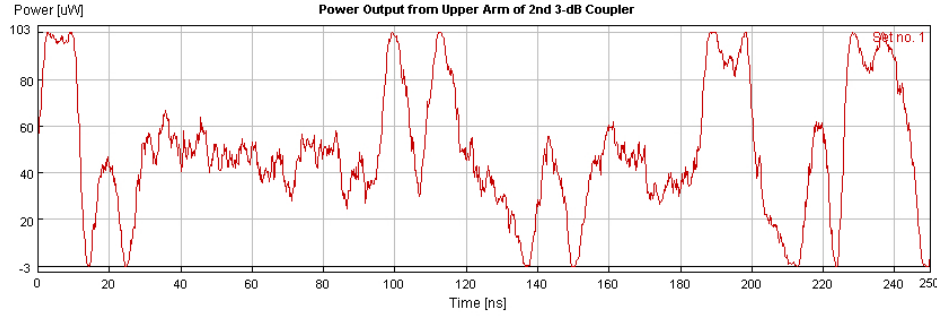
Figure 5.11e (-60 Degree Phase Shift)
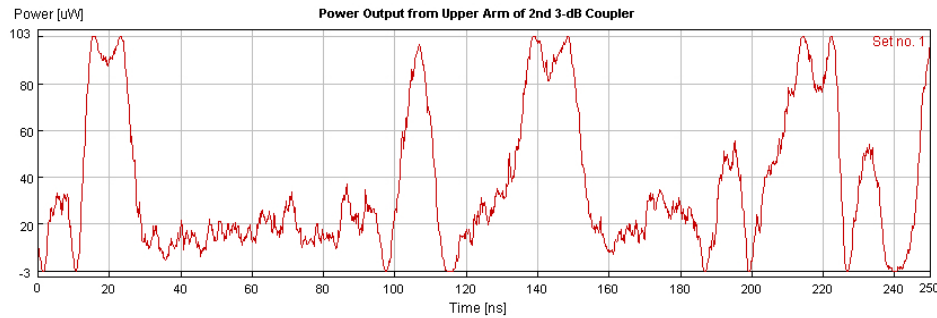
Figure 5.11f (57 Degree Phase Shift)
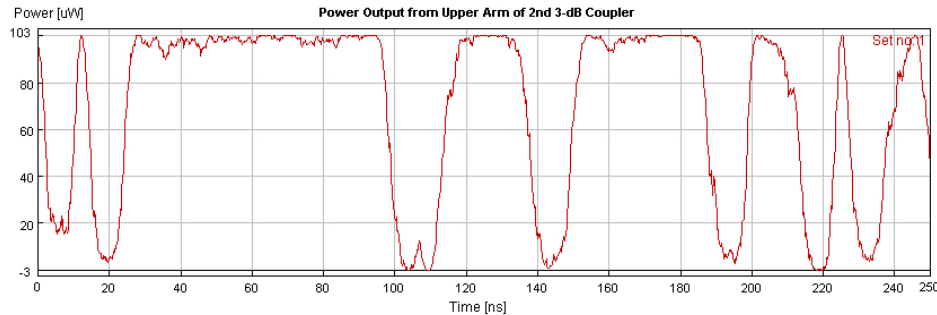
vi. The Effects of an Improper Bit Delay

Finally, the required precision of the optical delay can be predicted. Figure 5.12 shows simulation results using a laser with a linewidth of 1.5 MHz, ROP of 100 µW, and photodiode characteristics in table 5.2.   The proper delay at 80 Mb/s is 12.5 ns. Figure 5.12 shows that between 12.38 ns and 12.62 ns the receiver operated at a BER of 10^{-9} or better. For this particular receiver the delay must be within $\pm$ .12 ns. The delay is created by making the path in the upper arm longer than the path in the lower arm. A signal in fiber propagates at $2x10^8$ m/s. This corresponds to the delay needing to be accurate to within 24 mm. Figure 5.13 shows what the output bit stream looks like at various delays. Figure 5.13b shows that the output waveform matches the input of figure 5.13a. Figures 5.13c-5.13e show that the output becomes increasingly difficult to determine at imprecise delays. Figure 5.13f shows that if the delay is incorrect by a large amount it is possible for the output to be inverted.

Figure 5.12 (BER Dependence on Delay Time)
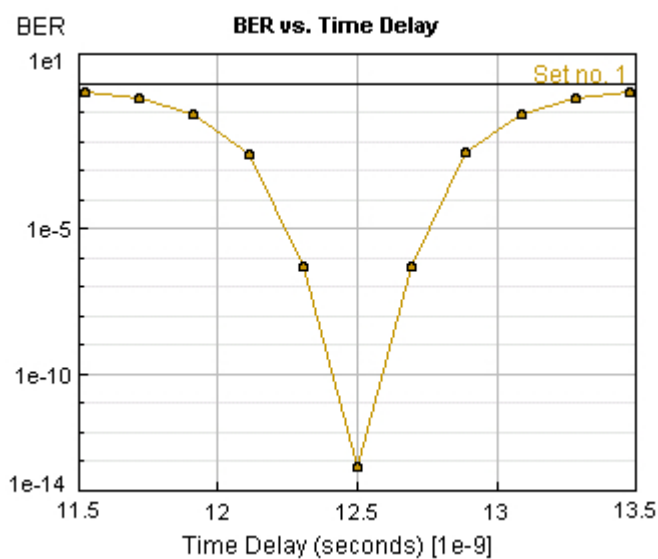
Figure 5.13a (Input Bit Stream)
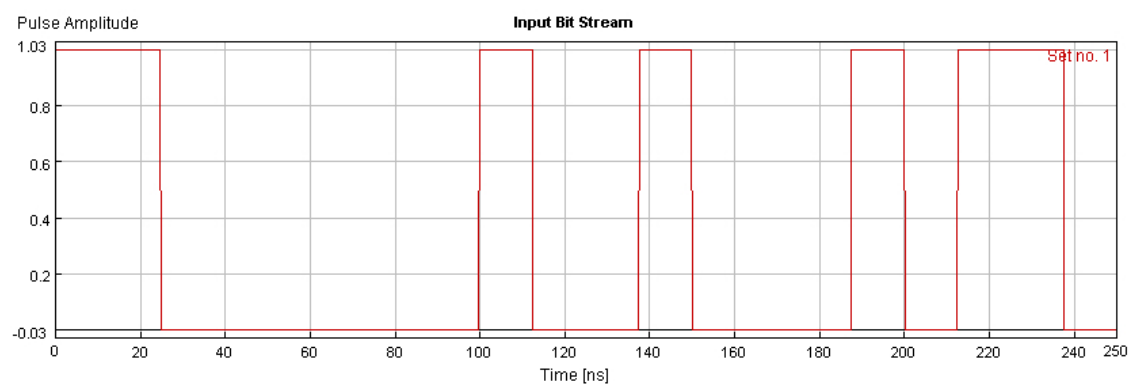
Figure 5.13b (12.5 ns Delay)
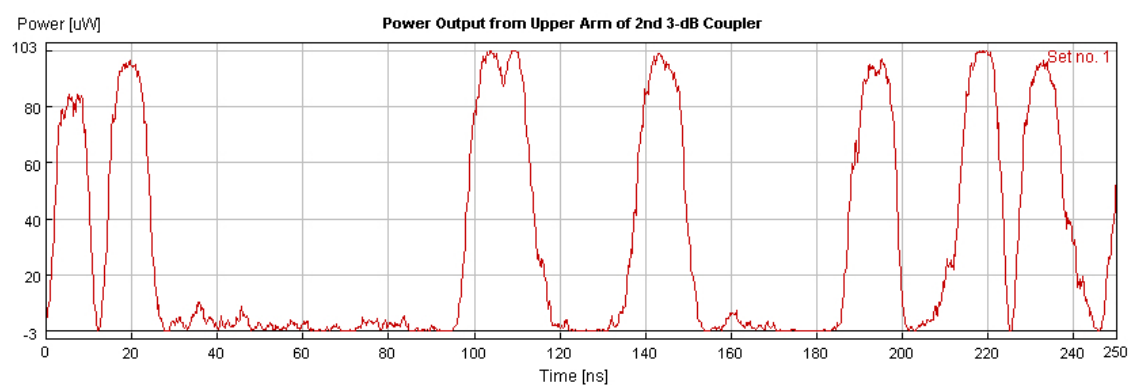
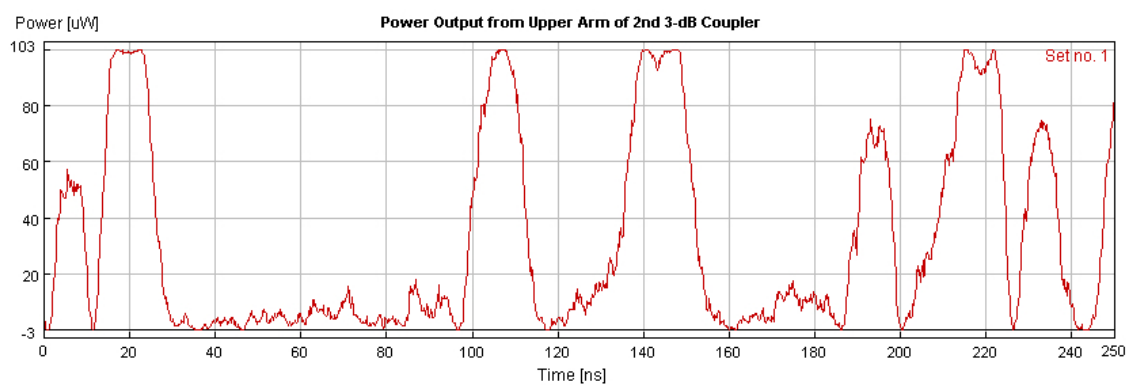Figure 5.13c (12.890625 ns Delay)

Figure 5.13d (13.671875 ns Delay)
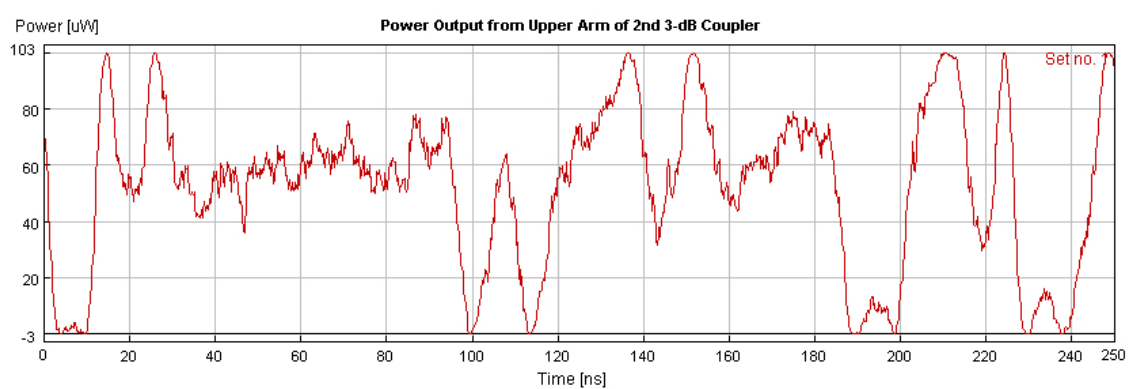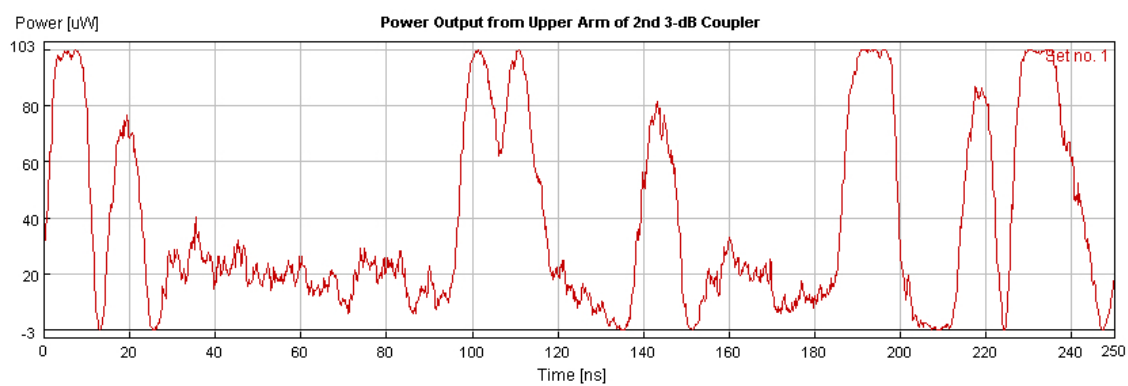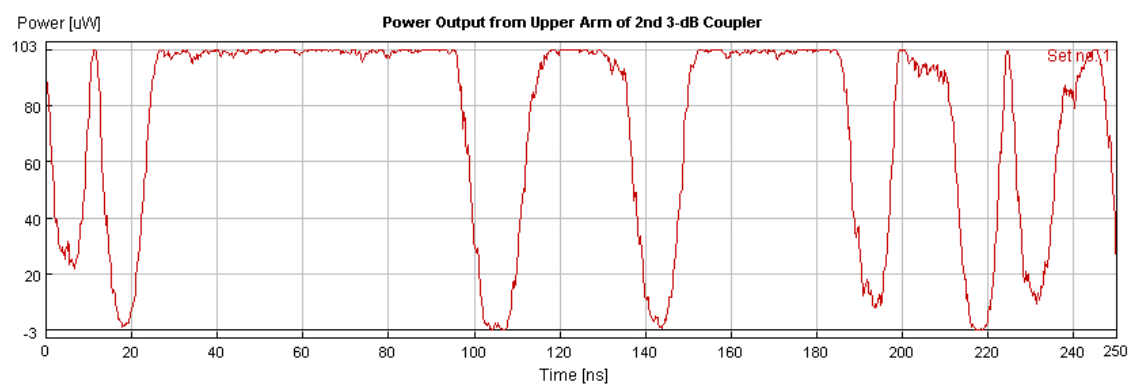

Figure 5.13e (12.109375 ns Delay)

Figure 5.13f (10.7421875 ns Delay)

Power Output from Upper Arm of 2nd 3-dB Coupler

VI. Hardware Verification

A. Coupler Power Splitting Observations

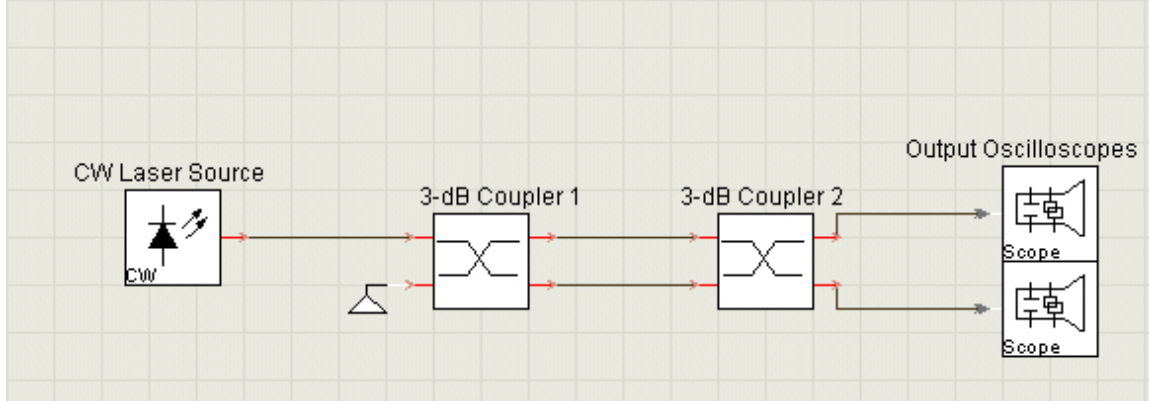Figure 6.1 (Cascading Coupler Setup for Power Splitting Observations)

Figure 6.1 is an experimental setup used to verify that proper power splitting occurs in the 3-dB couplers. It can be shown using the coupler equation in section II that the outputs of the second coupler in figure 6.1 are given by:

$$P_1 = 0 \tag{6.1}$$
$$P_2 = P_0 \tag{6.2}$$

In practice signals propagating in the region between the couplers wander in relative phase so that (6.1) and (6.2) become:

$$P_1 = \frac{P_0}{2}(1 - \cos(\Delta\phi_{random1}(t))) \tag{6.3}$$

$$P_2 = \frac{P_0}{2}(1 + \cos(\Delta\phi_{random2}(t))) \tag{6.4}$$

Where $\Delta\phi_{random1}(t)$ is the time varying random phase difference between the two arms of the interferometer. Lab measurements showed that the total power output from the second coupler is constant:

$$P_{3dB-Total} = P_1 + P_2. \tag{6.5}$$

However, observations of the power from either of the second coupler outputs was random over time. For the most part, the power output continuously varied, making it difficult to verify system operation. However, there were periods of a few seconds when the power out of each output was constant. This shows that this receiver is generally unstable but that there are brief instants of time where the output does stabilize. Steps were taken to counteract this instability as discussed in section VI part F.

B. Phase Modulator Observations

i. Suppressing Amplitude Modulation

Figure 6.2 (Experimental Setup Used to Verify Amplitude Modulation Suppression)
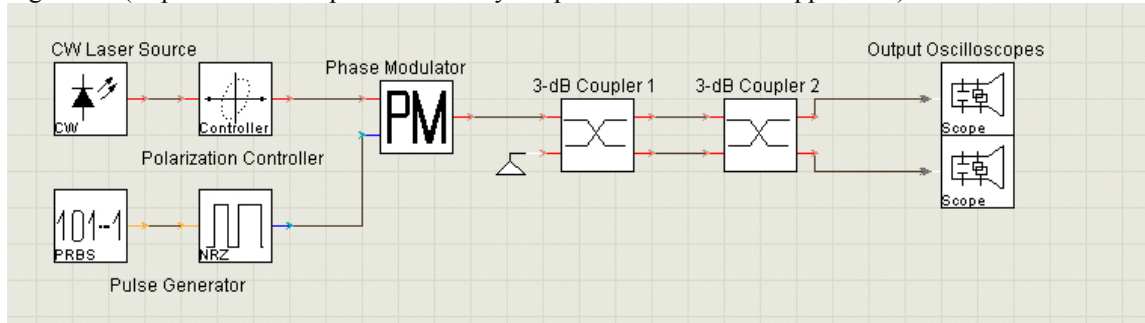
        It is difficult to verify that phase modulation is occurring. The electric field cannot be directly measured, only the optical power. Phase modulating a signal does not change its power so phase modulation cannot be observed at its output. It is not until after the second coupler that phase modulation becomes apparent when it is converted to power modulation. However, as established above, the power output from the second coupler is unstable due to random phase variations. This makes it difficult to determine if results are due to phase modulation or to random phase fluctuations. As described above the only way to determine if the phase modulator is working is to observe the output during the brief instants of system stability where the random phase variations are suppressed.
        To further complicate observing phase modulation, light must enter the phase modulator at a proper polarization angle in order for phase modulation to occur. If the polarization is incorrect then it is possible for the phase modulator to function as an amplitude modulator. The input to the phase modulator is polarization-maintaining and absorption reducing (PANDA) fiber. This type of optical fiber preserves the input polarization of a signal entering the phase modulator so that the polarization of light remains unchanged within the phase modulator. To ensure that light enters the phase modulator with the proper (SOP) a polarization controller immediately precedes the phase modulator. A polarization controller will rotate the polarization of an input to any desired output SOP.

36

Figure 6.3.a (No Amplitude Modulation)

Figure 6.3.b (Partial Amplitude Modulation)

Figure 6.3.c (Full Amplitude Modulation)

Figure 6.3 shows the effects of different input polarizations to the phase modulator. In figure 6.3a, the polarization has been adjusted until all amplitude modulation has been suppressed, in figure 6.3b, the polarization is only partially misaligned, causing partial amplitude modulation, and in figure 6.3c the input polarization to the phase modulator is completely misaligned so that amplitude modulation occurs.

ii. Phase Modulation Verification

Figure 6.4 (Setup Used to Verify Phase Modulation)
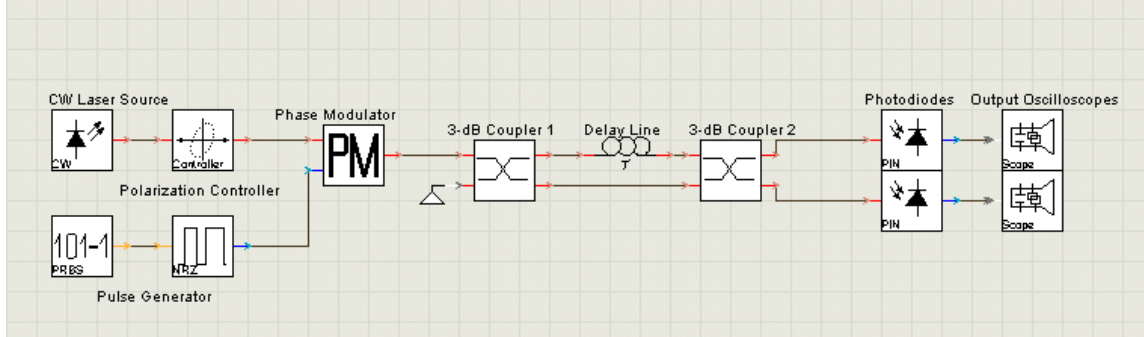
Figure 6.4 shows a lab setup used to verify phase modulation and coincidently also used to verify that the receiver is functioning properly. In this setup it is necessary to use a delay line to verify phase modulation. Without it there is no dependence on the phase modulated bit sequence to determine if phase modulation is occurring. (6.6) and (6.7) show the expected outputs in this setup are:

$$P_1 = \left(\frac{P_0}{2}\right)\left(1 - \cos(\Delta\phi d(t-\tau) - \Delta\phi d(t) - \tau\omega + \Delta\phi_{random1}(t))\right) \tag{6.6}$$

$$P_2 = \left(\frac{P_0}{2}\right)\left(1 + \cos(\Delta\phi d(t-\tau) - \Delta\phi d(t) - \tau\omega + \Delta\phi_{random2}(t))\right). \tag{6.7}$$

Experimental results showed that introducing a delay caused interference, showing that phase modulation was taking place. Without a delay no interference effects were present.

C. Proof of Proper Receiver Operation

In this sub-section, experimental results showing proper receiver operation are presented. Two different lasers are used to demonstrate this, laser "A" with an estimated linewidth between 1 to10 MHz and laser "B" with a 3 kHz linewidth. In the lab setup, the pulse generator does not possess the capability to differentially encode a sequence. Thus it is assumed that the output sequence of the pulse generator is already differentially encoded. The actual input sequence can be derived from the differential sequence by working backwards. All bit sequence figures below contain two bit patterns. Unless otherwise specified, the bit sequence on top corresponds to the input differential sequence from the pulse generator and the bottom sequence is the upper arm output from the second coupler. Figure 6.5 shows a differential sequence 1100001111000 used which yields an output sequence 1010001000100. The output sequence is delayed relative to the differential sequence because of a propagation delay. Working backwards from the differential sequence to find the true input sequence shows the two sequences to be the same. Hence proper receiver operation using laser "A" is demonstrated.

Figure 6.6 shows a result from a similar sequence, also using laser "A". The differential sequence is 100110 and as expected, the output sequence is 110101. The output of this figure is much clearer because the averaging feature of the oscilloscope has been used. This feature takes a specified number of samples and averages them to obtain a more stable waveform.

Figure 6.5 (Demonstration of Proper Receiver Operation Using Laser "A")
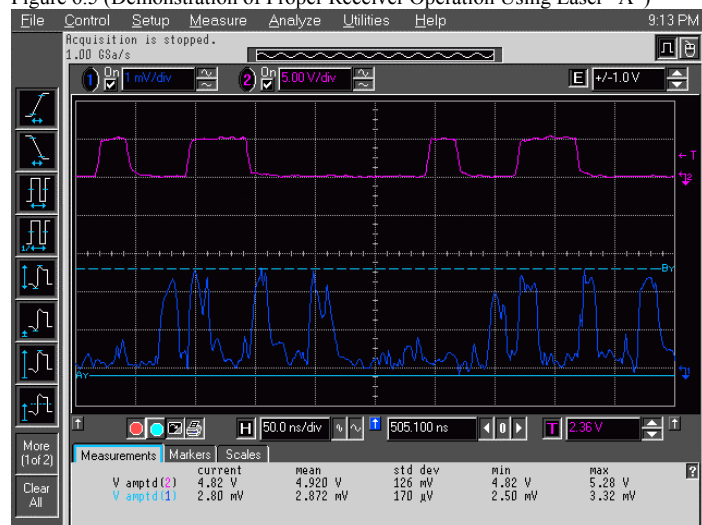

Figure 6.6 (Averaged Value Output using Laser "A")

In figure 6.5 it is clear that the output pulses have spread, which after comparing to the results in section V could result from either phase shift or delay mismatches. Figure 6.7 verifies that the receiver is working using laser "B". In this figure the DPSK coded sequence is: 0011110000101010000. This decodes to become 001000100001111111000 as shown in figure 6.7. In this figure it is clear that there is a phase shift error. The '1's in the output sequence have different amplitudes which is what the phase shift simulations showed. It is also clear in figure 6.7 that there is less phase noise. The output of laser "B" appears clearer than the output from laser "A" which is consistent with the linewidth of "B" being less than that of "A."

Figure 6.7 (Receiver Verification Using Laser "B")

D. Eye Diagrams

Figures 6.8 and 6.9 show eye diagrams generated using this laser. Eye diagrams are used to gauge system performance by combining the received 1's and 0's into the same plot. A closing
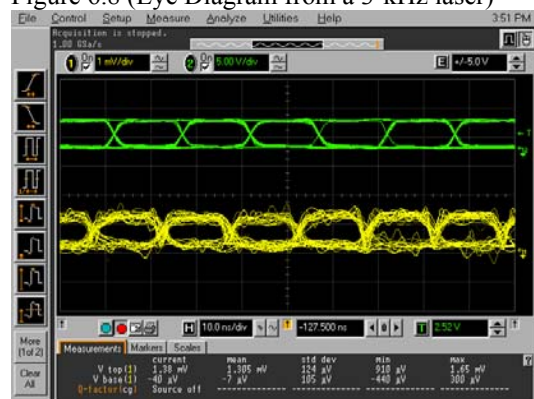
Figure 6.8 (Eye Diagram from a 3-kHz laser)

Figure 6.9 (Eye Diagram from a 3-kHz laser)

eye indicates degradation. From the Infinium Oscilloscope BER values could be calculated from the eye diagrams. Stability with this laser could only be achieved for a few seconds. Figure 6.8 shows an instant where the eye diagram is clean while figure 6.9 shows an instant where the quality of the eye is so poor that no opening is apparent. Clean eye openings could only be obtained for a few seconds. After this, the phasing effects of the receiver caused the output to become unstable. The Infinium Oscilloscope has the capability to average the voltages contained in 1's and in 0's and also computes the standard deviation of these quantities when a 2^{14}-1 PRBS bit sequence is used to generate the eye. Appendix D contains more eye figures. The Q value is computed from the eye and this is used to compute a BER. From the results of Appendix D the average Q value was 4.356, corresponding to a $6.942*10^{-6}$ BER.

E. Interference Maximization

Figure 6.10 (Experimental Setup used to Optimize Receiver Performance)
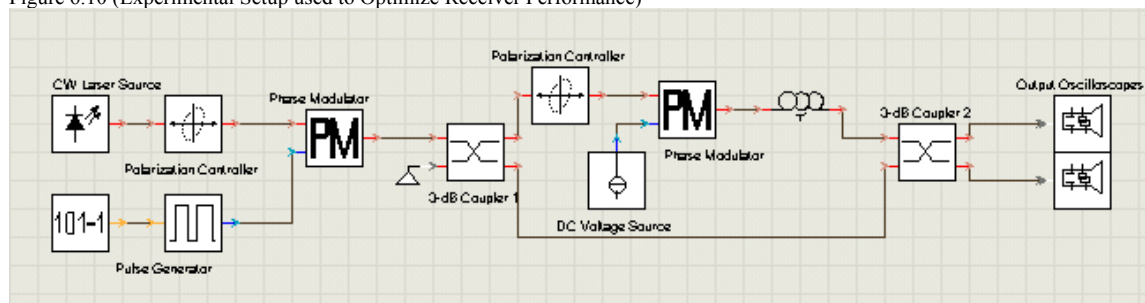
As discussed in section V the polarization of the two signals in the second 3-dB coupler needs to be identical for maximum interference to occur. To obtain maximum interference another polarization controller is added in the design, this time it is placed between the couplers in the arm where the delay line is located. Additionally, the second phase modulator discussed in section II and section V was added to maximize interference. By adjusting these devices the contrast ratio between 1's and 0's could be optimized. Figure 6.11 shows a result where the

Figure 6.11 (Sub-Optimum Contrast Ratio Obtained using Laser "B")
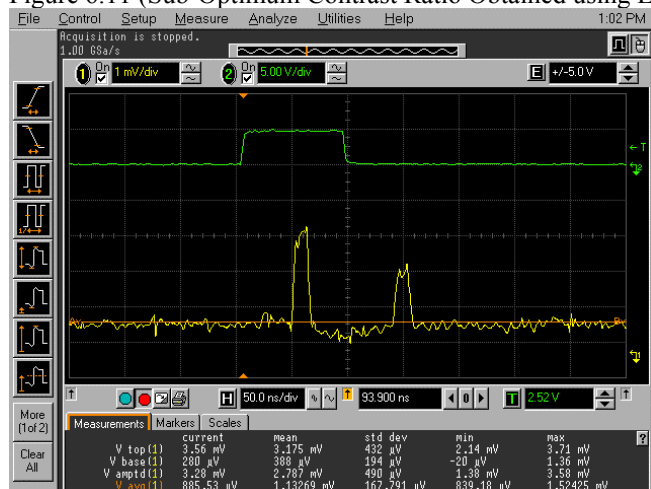
voltage in a '0' bit does not decrease all the way to 0 V. It was observed in lab work that the contrast ratio could be improved by adjusting the polarization controller and phase modulator. However, because of random phase fluctuations the improvement lasted for only fractions of a second.

F. The Setup

In computer simulations, laser linewidth was the biggest concern and was the dominant factor in determining receiver performance. Computer simulation assumed stable environmental conditions. In a lab setup, environmental conditions can have significant effects on the performance of optical receivers. The success of the DPSK demodulator depends on proper interference of light waves. Due to the precise phase and polarization required at the input to the second coupler the region between the two couplers is extremely sensitive to any disturbances,

which can change the phasing or polarization in this region. In order to get desired results at the output of the receiver it was necessary to put the setup on a floating table and then to cover the setup with a fiberglass case. The floating table isolated the receiver from any vibrations in the lab area. Additionally, all fiber within the setup was covered with clay to prevent movement of optical fiber, which could also cause phasing and polarization effects to disturb system performance. Enclosing the setup with a fiberglass box prevented the flow of air through the setup. The effect of these disturbances on the phase shift was analytically represented by the term $\Delta\phi_{random}$ in equations 6.6 and 6.7.

VII. Conclusion and Recommendations

The receiver described in this paper offers many advantages. It eliminates the need for a local oscillator, offers high receiver sensitivity compared to other modulation formats, and avoids excessive signal processing. The results of section VI demonstrated that for brief periods of time the receiver was stable. The instability of this system appears to be a result of the accumulation of phase noise and polarization instability. Due to the instability, it was difficult to properly set the delay, phase shift, or polarization to maximize system performance. As a result of this, the experimental BER values obtained from eye diagrams were lower than those obtained in simulation. Nonetheless, the receiver operated as expected under optimal conditions, verifying proof of principle. Considering the stringent linewidth requirements of the system at the data rate being used it is surprising that any performance verification occurred.

To obtain better results than achieved in this system, experimentation at higher data rates would reduce the linewidth requirements of the laser as proven in recent experiments elsewhere. It would also reduce the length of fiber needed to create a 1 bit delay so that less phase noise accumulates as the signal propagates in the delay arm. Using PANDA fiber throughout the whole communication system would stabilize the polarization. A phase locked loop that would control the relative phase of the signals before the second coupler would help to make the system stable. A more advanced approach to implement this design would be to use integrated optics. This would help to isolate the receiver from environmental factors that could effect receiver performance. A form of DPSK known as Differential Quadrature Phase Shift Keying (DQPSK) has shown success at 10 Gb/s using integrated optics. [19] Recent demonstration of record transmission distances using a DPSK format show the relevance of this communication system to current research. [3]

Bibliography

[1]   R Gagliardia and S Karp, *Optical Communications*. John Wiley & Sons, 1976.

[2]   F.G. Stremler: "Introduction to Communication Systems"; 3Rd Ed, Addison-Wesley, 1992.

[3]   A.H. Gnauck, G. Raybon, S. Chandrasekhar, *et al*. "2.5 Tb/s (64 x 42.7 Gb/s) Transmission over 40 x 100 km NZDSF Using RZ-DPSK Format and All-Raman-Amplified Spans," *OFC 2002 Post deadline Paper*, FC2.

[4]   K. Kiasaleh, "An All Optical Coherent Receiver for Self-Homodyne Detection of Digitally Phase Modulated Signals," *IEEE Transactions on Communications,* vol. 42, no. 2/3/4, pp. 1496-1500, Feb/Mar/Apr. 1994.

[5]   R. Vodhanel, "5 Gbit/s Direct Optical DPSK Modulation of a 1530-nm DFB Laser," *IEEE Photonics Technology Letters,"* vol. 1, no. 1, pp. 218-220, Aug. 1989.

[6]   I. Bar-David, "Direct Differential Detection of Phase-Shift-Keyed Signals: a Local-Oscillatorless DPSK receiver," *IEE Proceedings of Opto-Electronics,* vol. 141, no. 1, pp. 38-42, Feb. 1994.

[7]   L Kazovsky, "Decision-Driven Phase-Locked Loop for Optical Homodyne Receivers: Performance Analysis and Laser Linewidth Requirements" *Journal of Lightwave Technology,* vol. LT-3, no. 6, pp. 1238-1247. Dec. 1985.

[8]   L Kazovsky, "Performance Analysis and Laser Linewidth Requirements for Optical PSK Heterodyne Communications Systems" *Journal of Lightwave Technology,* vol. LT-4, no. 4, pp. 415-425, Apr. 1986.

[9]   L Kazovsky, "Balanced Phase-Locked Loops for Optical Homodyne Receivers: Performance Analysis, Design Considerations, and Laser Linewidth Requirements " *Journal of Lightwave Technology,* vol. LT-4, no. 2, pp. 182-195, Feb. 1986.

[10]   L. Kazovsky, "Optical Heterodyning Versus Optical Homodyning: a comparison," *Journal of Optical* Communications vol. 6 no. 1, pp. 18-24, 1985.

[11]   J.M. Kahn, I.M.I. Habbab, and C.R. Giles, "1 Gbit/s Zero-IF DPSK Coherent Optical System Using a Single Photodetector" *Electronics Letters* vol. 24 no. 23, pp. 1455-1456.

[12]   M. Tateda, S. Seikai, and N. Uchida, "Phase-Modulated Optical Signal Detection by Retardation Method," *IEEE Journal of Quantum Electronics*, vol. QE-19, no. 1, pp. 96-100.

[13]   Performance of Novel Low Intermediate Frequency Coherent Optical DPSK Receiver Using Baseband Detection," vol. 138, no. 6 Dec. 1991 pp. 401-411.

[14]   G. Keiser, *Optical Fiber Communications,* 3rd Ed. McGraw-Hill, 2000.

[15]   VPI BER Training Manual

[16]   G. Agrawal and N. Dutta, *Long Wavelength Semiconductor Lasers*. Van Nostrand Reinhold Company, 1986.

[17]   J. Gowar, *Optical Communication Systems (379-400)*. Prentice Hall, 1984.

[18]   VPI Photonic Modules Reference Manual II.

[19]   R.A. Griffin, *et al*. "10 Gb/s Optical Differential Quadrature Phase Shift Key (DQPSK) Transmission using GaAs/AlGaAs Integration," *OFC 2002 Post deadline Paper,* FD6-1.

Appendix A

Description of a White Noise Process

The probability density function (PDF) of a white noise process is defined by:

$$p(x) = \frac{1}{\sigma\sqrt{2\pi}} e^{-(1/2)[(x-\mu)/\sigma]^2} \qquad -\infty < x < \infty \tag{A.1}$$

where x is the value of a random variable. The integral from a to b of $p(x)$ is the probability that the random variable takes on a value in [a,b], where μ is the mean of x, and σ is the standard deviation of x as shown in figure A.1 with $\mu = 0$ and $\sigma = 1$. [1]

Figure A.1 (PDF for a White Noise Process)
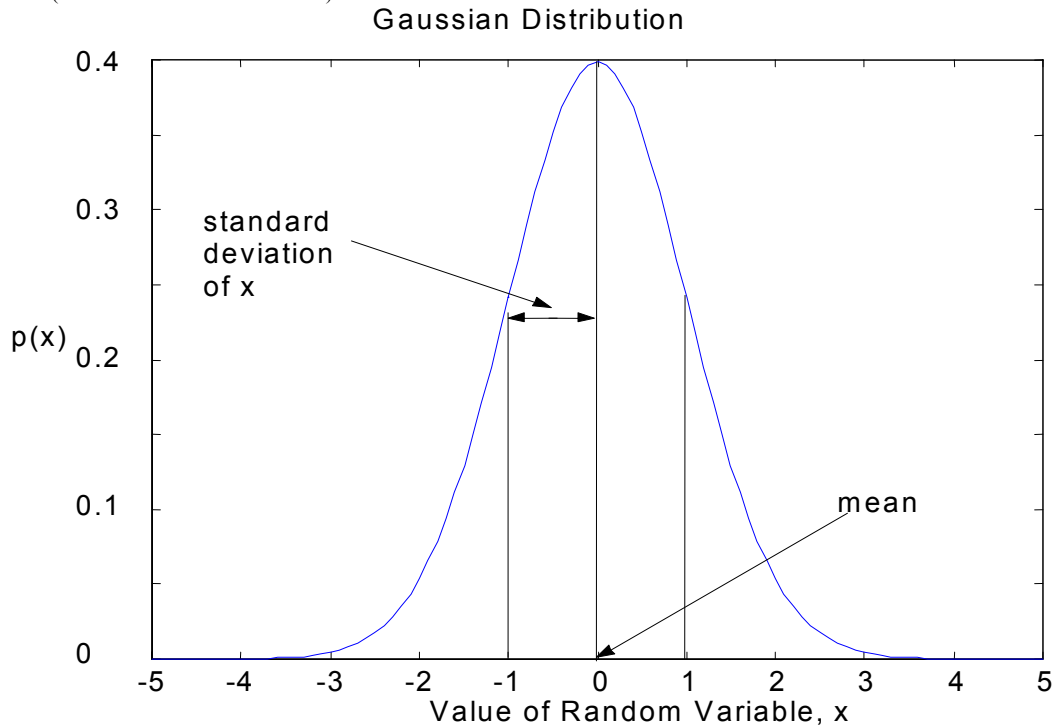
Dispersion [2]

Dispersion is the spreading of a pulse in time as it propagates within an optical fiber. Figure A.2 illustrates this. Dispersion results from the frequency dependence of β. Its frequency dependence can be shown by a Taylor expansion about a frequency ω_0 so that:

$$\beta(\omega) = \beta_0(\omega_0) + \beta_1(\omega_0)(\omega - \omega_0) + \frac{1}{2}\beta_2(\omega_0)(\omega - \omega_0)^2 + \frac{1}{6}\beta_3(\omega_0)(\omega - \omega_0)^3 + ...$$
$$+ \frac{1}{n!}\beta_n(\omega_0)(\omega - \omega_0)^n \tag{A.2}$$
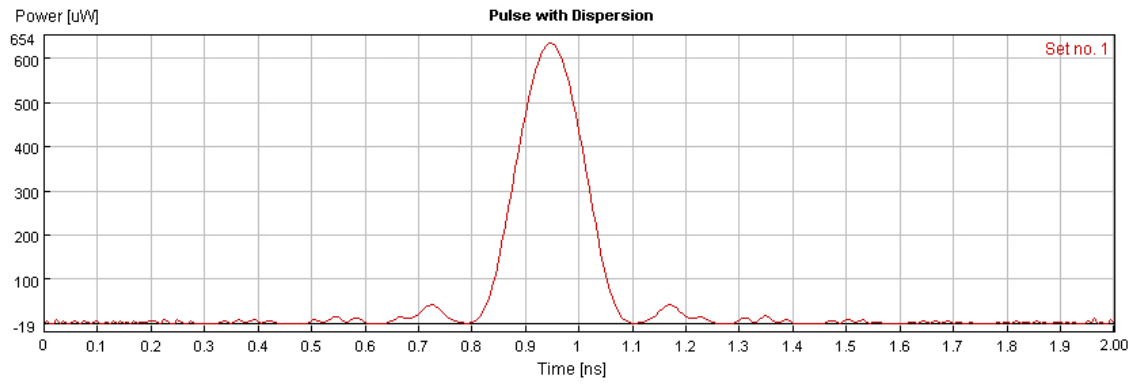
Figure A.2.a (Pulse without Dispersion)
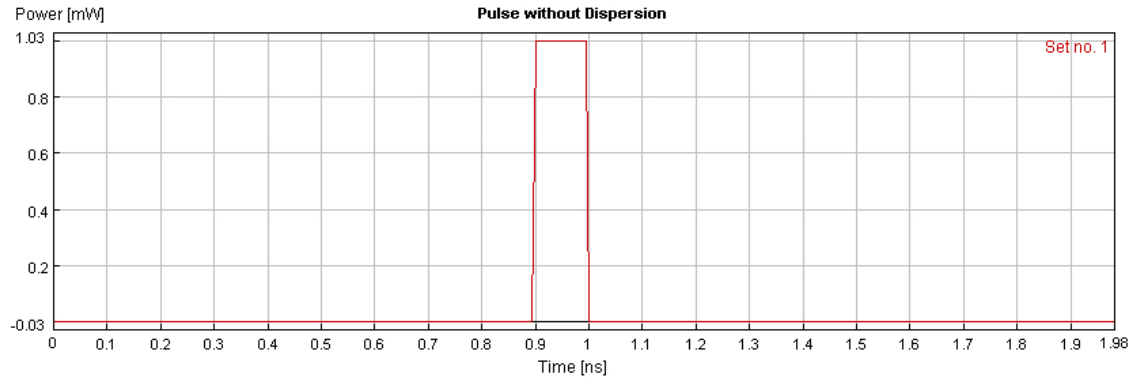
Figure A.2.b (Pulse with Dispersion)

where $\beta_m = (\dfrac{\partial^n \beta}{\partial \omega^n})\Big|_{\omega=\omega_0}$. Only the second and third order terms in this expansion contribute

significantly to dispersion so all other terms are ignored. These terms correspond to second and third order dispersion respectively. The expressions for these terms are given by:

$$\beta_2 = -\frac{D\lambda^2}{2\pi c} \tag{A.3}$$

$$\beta_3 = \frac{\lambda^2}{(2\pi c)^2}(\lambda^2 S_0 + 2\lambda D) \tag{A.4}$$

In these expressions D is the dispersion and S_0 is the dispersion slope, related to D by:

$$S_0 = \frac{\delta D}{\delta \lambda} \tag{A.5}$$

[1] R. Walpole, R. Myers, S. Myers, *Probability and Statistics for Engineers and Scientists* 6th Ed Prentice Hall, 1998.
[2] G Keiser, *Optical Fiber Communications* 3rd Ed McGraw-Hill, 2000.

Appendix B

Figures B.1-B.9 on the following pages show eye diagrams generated from an Infinium Oscilloscope. On each of these figures two eye diagrams are shown. Each pair of eye diagrams corresponds to both outputs. The following results present calculations based on the lower eye diagram in figure B.1-B.9. The lower eye corresponds to the output from upper arm photodiode. From these eye diagrams the Q value and then the BER can be calculated using (4.3) and (4.4). A sample calculation from Figure B.1 corresponding to Q_1 is shown here. Table B.1 shows the results from different eye diagrams.

Sample Calculation:

$$Q_1 = \frac{|\mu_1 - \mu_0|}{\sigma_1 + \sigma_0} = \frac{|2.720mV - 756\mu V|}{140\mu V + 378\mu V} = 3.79 \quad BER = \frac{1}{\sqrt{2\pi}}\frac{e^{-Q^2/2}}{Q} = \frac{1}{\sqrt{2\pi}}\frac{e^{-(3.79)^2/2}}{3.79} = 79.36*10^{-6}$$

Table B.1 (BER Results)

Eye Diagram	μ_1 (mV)	μ_1 (μV)	σ_1 (μV)	σ_0 (μV)	Q	BER
Q_1	2.720	756	140	378	3.792	$79.36*10^{-6}$
Q_2	2.631	523	123	260	5.504	$19.14*10^{-9}$
Q_3	2.723	785	149	617	2.530	$6.425*10^{-3}$
Q_4	2.684	539	140	483	3.443	$30.89*10^{-3}$
Q_5	2.697	523	113	378	4.428	$4.978*10^{-6}$
Q_6	2.680	724	130	264	4.964	$358.3*10^{-9}$
Q_7	2.683	696	144	349	4.030	$29.44*10^{-6}$
Q_8	2.713	545	138	288	5.089	$186.5*10^{-9}$
Q_9	2.732	627	137	251	5.425	$29.90*10^{-9}$
Avg					**4.356**	

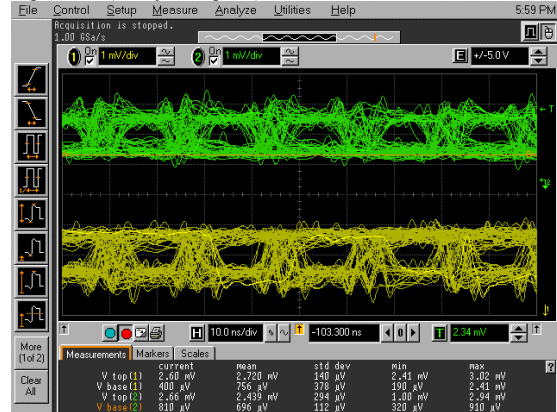Using the average Q value to compute the BER gave a value of **$6.942*10^{-6}$**

Figure B.1 (Q_1 Eye Diagram)

Figure B.2 (Q_2 Eye Diagram)
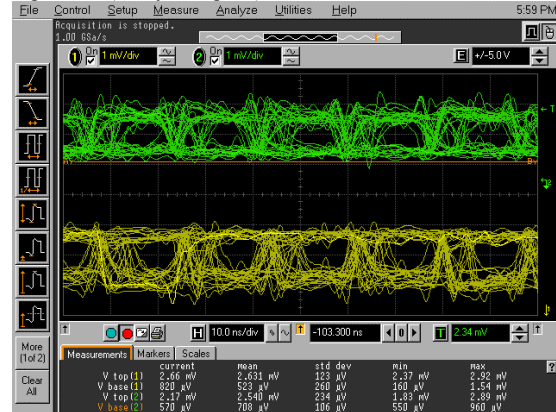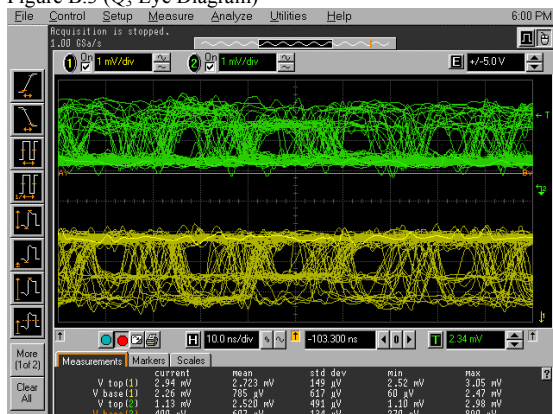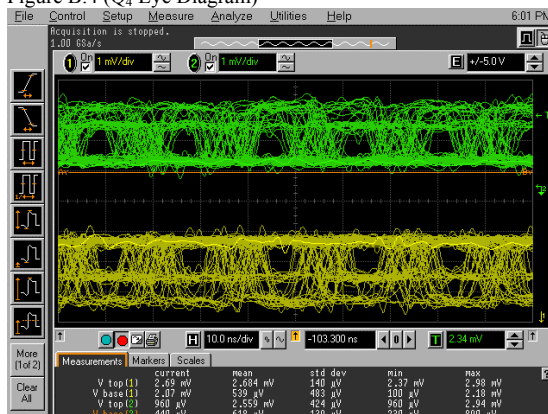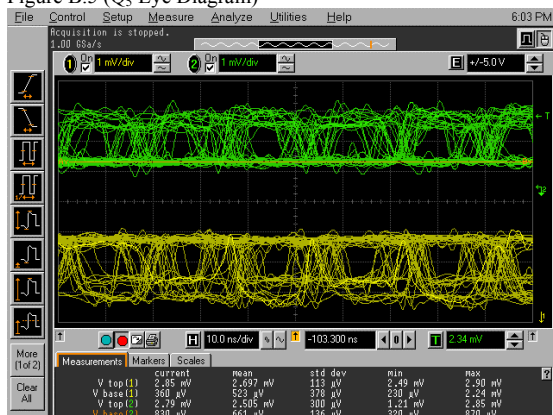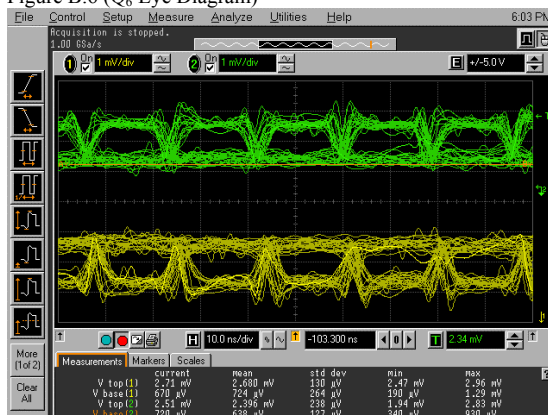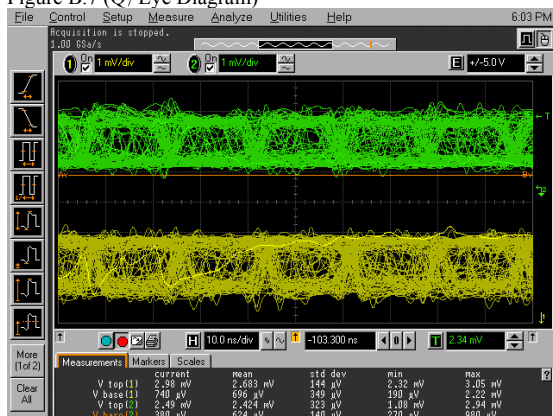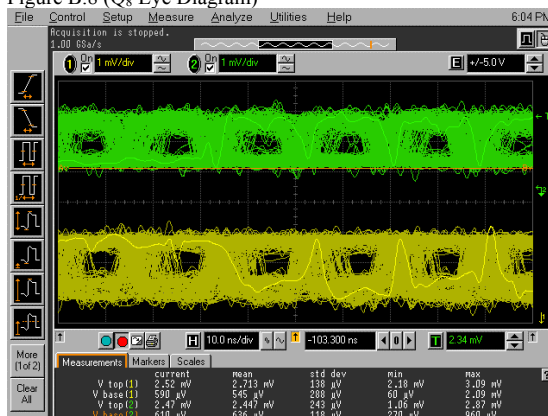
Figure B.3 (Q_3 Eye Diagram)

Figure B.4 (Q_4 Eye Diagram)

Figure B.5 (Q_5 Eye Diagram)

Figure B.6 (Q_6 Eye Diagram)

Figure B.7 (Q_7 Eye Diagram)

Figure B.8 (Q_8 Eye Diagram)

Figure B.9 (Q_9 Eye Diagram)